The reflectivity method: a tutorial

G. Müller

Institute of Meteorology and Geophysics, University of Frankfurt, Feldbergstr. 47, 6000 Frankfurt,
Federal Republic of Germany

Abstract. An extended reflectivity method is described
by which complete seismograms for a point source in a
layered half-space can be calculated. Starting with the
differential equations and boundary conditions, the re-
flection and transmission of plane waves at layered me-
dia is treated first, followed by the synthesis of point-
source wave fields. The frequency-domain displace-
ments of the half-space surface are expressed as slow-
ness integrals, and the most prominent parts of the in-
tegrands are the reflectivities of the layers below and
above the point source and a function which is closely
related to the transmissivity of the layers above the
source. Reflectivities and transmissivities are calculated
by recursive methods which are numerically stable for
all frequencies and slownesses. Near- and far-field re-
sults are given for single-force and moment-tensor
point sources. From the general results for the com-
plete medium response, partial responses can easily be
extracted, e.g. the original form of the reflectivity meth-
od which calculates only the response from the layers
below the source. Thus, the extended reflectivity meth-
od has a flexibility which is not available if propagator
methods are used for the calculation of the integrands.
Various other aspects of seismogram calculation are
addressed, such as extended sources, an earth-flattening
transformation and the inclusion of absorption for con-
stant and frequency-dependent Q. Theoretical seismo-
grams are shown, first for body-wave propagation from
explosions in a crustal model and in a model which
came from seismic prospecting, and second for surface-
wave propagation from a double-couple source.

Due to the tutorial nature of this paper the de-
rivations are mostly rather detailed. It is hoped that
this will help interested newcomers to the field of
theoretical seismograms to get started.

Key words: Reflectivity method – Reflection and trans-
mission coefficients – Synthetic seismograms – Dissi-
pation

1. Introduction

The theory of seismic wave propagation in horizontally
stratified media, i.e. in media whose elastic and anelas-
tic properties depend only on depth, has been a main
subject of research in seismology over the past decades.

Currently, however, the interest of seismologists and
theoreticians focuses strongly on methods which allow
the treatment of laterally heterogeneous media. This de-
velopment has been prompted by many clear percep-
tions, collected in several disciplines of geosciences, that
the earth is a dynamic body with relatively rapid in-
ternal motions. These processes and related horizontal
temperature differences may lead to pronounced lateral
variations in elastic and anelastic properties. Thus, for
the seismologist, who is interested in depth ranges from
the lower crust to the core, the earth becomes what it
has always been for those engaged in seismic prospect-
ing: a medium with truly three-dimensional inhomo-
geneities.

Methods for horizontally stratified earth models
will, of course, continue to have their importance and
find applications in studies of structural properties and
sources of seismic waves. Hence, a good understanding
of the relevant theory will always be a necessity. The
purpose of these lecture notes is to contribute to this
understanding by presenting a self-contained theory of
one of the methods for horizontally layered media, the
reflectivity method, including all material that is neces-
sary for the development of corresponding computer
programs for theoretical seismograms.

Before we start with the details, a few words about
the general scene of methods for horizontally stratified
media are in order. This scene is very vast now, and it
is practically impossible to mention all the different
methods that are in use. Much background material
can be found in the text books and monographs by Pi-
lant (1979), Aki and Richards (1980), Ben-Menahem
and Singh (1981) and Kennett (1983). The most impor-
tant theories and methods for wave propagation and
seismogram synthesis are the following (the references
given are only examples and far from complete):
Generalized ray theory (Helmberger, 1968; Müller,
1969; Ben-Menahem and Vered, 1973): the medium is
approximated by homogeneous layers, and the wave
field is decomposed into elementary seismograms corre-
sponding to rays.
Full-wave theory (Cormier and Richards, 1977): a ray
theory for inhomogeneous layers which takes account
of frequency-dependent effects connected, e.g., with
caustics and shadow zones.
WKBJ theory (Chapman, 1978): a ray theory for in-
homogeneous layers which is more limited than full-

wave theory, as far as frequency-dependent effects are concerned, but which allows very rapid computations.

Wavenumber or slowness integration methods (Kind, 1978; Cormier, 1980; Wang and Herrmann, 1980; Ingate et al., 1983; Ha, 1984): representation of the Fourier-transformed wave field of a layered medium by integrals over horizontal wavenumber or slowness; the reflectivity method belongs to this class of methods (see below).

Wavenumber summation methods (Alekseev and Mikhailenko, 1980; Bouchon, 1981; Korn and Müller, 1983; Spudich and Ascher, 1983; Olson et al., 1984; Campillo et al., 1984): both time- and frequency-domain methods which are in principle very similar to wavenumber integration methods, but the continuous distribution of wavenumbers is replaced by a discrete one.

Modal summation method (Harvey, 1981; Panza, 1985): representation of the wave field by normal modes of Rayleigh and Love waves alone, either with the assumption of a perfect reflector at depth or without.

The first three of these methods are suitable for the calculation of body-wave contributions to seismograms, whereas the last three also allow surface waves to be included, i.e. these methods are methods for complete seismograms.

The *reflectivity method*, which is described below in more detail, is a wavenumber or slowness integration method. The name stems from the fact that the function which is integrated is mainly the reflection coefficient or reflectivity of a layered medium. At first, this is true only for a layered medium without a free surface and with a source on one side of those layers whose reflections are sought; this is the geometry for which the reflectivity method was developed originally (Fuchs, 1968; Fuchs and Müller, 1971). However, Kennett and Kerry (1979) and Kennett (1983) have shown that in the case of a layered half-space, having a free surface and a source at arbitrary depth, the integrand of the wavenumber or slowness integrals can be expressed mainly by the reflectivities of two partitions of the medium – the layers above the source and those below. This form of the theory justifies the continued use of the name reflectivity method. However, we emphasize that there is no difference to the wavenumber or slowness integration methods quoted above in which the integrand is calculated differently, namely by matrix or propagator techniques. That notations here indeed have a certain degree of arbitrariness, is illustrated by the fact that Luco and Apsel (1983) and Apsel and Luco (1983), whose treatment of the layered half-space comes closest to the results presented below, call their method simply a wavenumber-integration method.

These lecture notes are organized as follows. After a discussion of the differential equations for wave propagation in horizontally stratified media and of the boundary conditions in Section 2, we derive in Section 3 the reflection and transmission coefficients (or reflectivities and transmissivities) for plane waves, incident on a plane interface or a stack of homogeneous layers separating two homogeneous half-spaces. The coefficients for an interface are given analytically and those for a stack of layers are derived by a recursive algorithm first described by Kennett (1974). In Section 4 we start with the displacement potentials for a point source in a homogeneous medium and their well-known representation by Sommerfeld integrals in the wavenumber or slowness domain. Similar representations are valid for the displacement components at points with arbitrary location in a layered medium. The upgoing wave field in the layer with the source is synthesized as the sum of the direct wave from the source and all possible interactions between the layer stack above the source and that below the source. The interaction terms contain the reflectivities of these zones: in the case of $P - SV$ waves, they are 2×2 matrices whose elements are the $P - P$, $SV - P$, $P - SV$, $SV - SV$ reflection coefficients; in the case of SH waves, they are scalars. The upgoing wave field in the source layer is then transmitted through the layer stack above the source with the aid of the transmissivity of this zone, and the complete wave field in the half-space on top of the medium is obtained. An analytical limiting process which turns this half-space into vacuum gives, for points on the uppermost interface, the final expressions for the displacement components. The basic ideas of this wave field synthesis follow Kennett and Kerry (1979) and Kennett (1983), but some details are different – mainly the treatment of transmission through the layers above the source. The theory is presented here for the simplest type of point source, radiating P, SV and SH waves, a single force of arbitrary orientation. Final results for a general moment-tensor point source, including an explosion, are also given.

In Section 5 we discuss the possibility of extracting, from the expressions for the complete wave field, simpler expressions which represent only partial responses of the layered medium. Moreover, compact far-field formulas for extended sources consisting of several point sources are compiled, and a few computational aspects of the reflectivity method are mentioned. Section 6 first presents an earth-flattening transformation by which the reflectivity method can also be used for media with spherical geometry; it is adequate for many body and surface waves propagating in a spherical earth. Then we describe how the theory of wave propagation for purely elastic media is modified for dissipative media. Under the usual, experimentally confirmed assumption of a linear relation between stress and strain also in dissipative media at low strains, these media are completely described by complex elastic moduli and hence by complex wave velocities. A few possibilities of choosing these velocities, according to non-causal or causal absorption, are described. Finally, in Section 7 we present results of some synthetic-seismogram calculations.

2. Differential equations and boundary conditions

We assume that the medium consists of homogeneous layers, separated by first-order discontinuities. If a medium is continuously inhomogeneous (throughout or piecewise), it is replaced by a sufficiently large number of homogeneous layers; in smooth gradient zones it is usually enough to choose roughly half the dominant wavelength as layer thickness, whereas in transition zones with larger velocity gradients the layer thickness

should be reduced further. The advantage of the homogeneous-layer approximation is that inside each layer the equation of motion takes a relatively simple form. Its disadvantage is that boundary conditions have to be fulfilled at many interfaces. *Analytical* methods for inhomogeneous layers (in contrast to numerical, e.g. finite-difference, methods) are not yet developed to a point where they really can compete with the methods for homogeneous layers.

The equation of motion of a homogeneous, isotropic elastic medium is

$$\rho \mathbf{u}_{,tt} = (\lambda + 2\mu)\,\text{grad div}\,\mathbf{u} - \mu\,\text{rot rot}\,\mathbf{u}, \tag{1}$$

where $\mathbf{u}$ is the displacement vector, ρ the density and λ and μ the Lamé parameters. Body forces due to gravity and seismic sources are not included in Eq. (1): it is assumed that gravity has no other effect than to determine, via self-compression, the (constant) values of ρ, λ and μ, and sources of seismic waves are included through their known contributions to $\mathbf{u}$ (see Section 4).

Next we introduce *displacement potentials*, from which the displacements follow by spatial differentiation. For the first case of reflection and transmission that we consider later, i.e. reflection and transmission of plane waves (Section 3), we use *Cartesian coordinates* (x, y, z), place the interfaces at constant values of z and assume independence of the y coordinate. Then it is most appropriate to derive the displacements u_x and u_z from potentials ϕ and ψ:

$$u_x = \phi_{,x} - \psi_{,z}, \qquad u_z = \phi_{,z} + \psi_{,x}. \tag{2}$$

For the displacement u_y, no potential is used. Inserting the corresponding representation of the displacement vector

$$\mathbf{u} = \text{grad}\,\phi + \text{rot}(\mathbf{e_y}\,\psi) + \mathbf{e_y}\,u_y \tag{3}$$

($\mathbf{e_y}$ = unit vector in y-direction) into Eq. (1), one obtains *wave equations* for ϕ, ψ and u_y:

$$\nabla^2 \phi = \frac{1}{\alpha^2}\phi_{,tt}, \qquad \nabla^2 \psi = \frac{1}{\beta^2}\psi_{,tt}, \qquad \nabla^2 u_y = \frac{1}{\beta^2}u_{y,tt}. \tag{4}$$

Here, $\nabla^2 = \partial^2/\partial x^2 + \partial^2/\partial z^2$ is the Laplace operator in two dimensions, $\alpha = [(\lambda + 2\mu)/\rho]^{1/2}$ the velocity of P waves and $\beta = (\mu/\rho)^{1/2}$ the velocity of S waves. Equations (4) imply decoupled propagation of P and S waves within the layers.

In the second case considered below, reflection and transmission of waves from a point source (Section 4), *cylindrical coordinates* (r, φ, z) are most appropriate. Then we use displacement potentials for *all* displacement components and obtain instead of Eqs. (2) and (3) ($\mathbf{e_z}$ = unit vector in z-direction):

$$\mathbf{u} = \text{grad}\,\phi + \text{rot rot}(\mathbf{e_z}\,\Psi) + \text{rot}(\mathbf{e_z}\chi) \tag{5}$$

$$\begin{aligned}
u_r &= \phi_{,r} + \Psi_{,rz} + \frac{1}{r}\chi_{,\varphi}\\
u_\varphi &= \frac{1}{r}\phi_{,\varphi} + \frac{1}{r}\Psi_{,\varphi z} - \chi_{,r}\\
u_z &= \phi_{,z} - \Psi_{,rr} - \frac{1}{r}\Psi_{,r} - \frac{1}{r^2}\Psi_{,\varphi\varphi}.
\end{aligned} \tag{6}$$

By inserting Eq. (5) into Eq. (1), again wave equations are found, this time for all potentials:

$$\nabla^2 \phi = \frac{1}{\alpha^2}\phi_{,tt}, \qquad \nabla^2 \Psi = \frac{1}{\beta^2}\Psi_{,tt}, \qquad \nabla^2 \chi = \frac{1}{\beta^2}\chi_{,tt}. \tag{7}$$

The second of these equations can be used to simplify the displacement component u_z in Eq. (6):

$$u_z = \phi_{,z} + \Psi_{,zz} - \frac{1}{\beta^2}\Psi_{,tt}. \tag{6'}$$

The *boundary conditions* require continuity of the traction and displacement vectors across internal interfaces in solid media. At a free surface the traction vanishes, and the displacements are unspecified.

If *Cartesian coordinates* are used, the traction components, i.e. normal and tangential stresses, are:

$$p_{zx} = \mu(u_{z,x} + u_{x,z}), \qquad p_{zy} = \mu u_{y,z}, \qquad p_{zz} = \lambda\,\text{div}\,\mathbf{u} + 2\mu u_{z,z}.$$

Inserting Eq. (2) here, we obtain the first three boundary conditions which require continuity of the quantities

$$\mu\left(2\phi_{,xz} - 2\psi_{,zz} + \frac{1}{\beta^2}\psi_{,tt}\right), \qquad \mu u_{y,z'}$$

$$\frac{\lambda}{\alpha^2}\phi_{,tt} + 2\mu(\phi_{,zz} + \psi_{,xz}) \tag{8a}$$

at all interfaces, including a free surface where these quantities vanish. The conditions for displacements at internal interfaces additionally require continuity of the quantities

$$\phi_{,x} - \psi_{,z}, \qquad u_y, \qquad \phi_{,z} + \psi_{,x}. \tag{8b}$$

In the case of *cylindrical coordinates*, the relevant stresses are

$$p_{zr} = \mu(u_{z,r} + u_{r,z}), \qquad p_{z\varphi} = \mu\left(u_{\varphi,z} + \frac{1}{r}u_{z,\varphi}\right),$$

$$p_{zz} = \lambda\,\text{div}\,\mathbf{u} + 2\mu u_{z,z}.$$

Inserting Eqs. (6) and (6'), one finds those quantities which are continuous at interfaces, in analogy to Eqs. (8a) and (8b). These quantities are not reproduced here. Closer inspection shows that they are continuous if the simpler quantities

$$\mu\left(\phi_{,z} + 2\Psi_{,zz} - \frac{1}{\beta^2}\Psi_{,tt}\right),$$

$$\mu\chi_{,z}, \qquad \frac{\lambda}{\alpha^2}\phi_{,tt} + 2\mu\left(\phi_{,zz} + \Psi_{,zzz} - \frac{1}{\beta^2}\Psi_{,ttz}\right) \tag{9a}$$

and

$$\phi + \Psi_{,z}, \qquad \chi, \qquad \phi_{,z} + \Psi_{,zz} - \frac{1}{\beta^2}\Psi_{,tt} \tag{9b}$$

are continuous; these quantities contain no derivatives with respect to the horizontal coordinates r and φ. For instance, if the first two functions in Eq. (9b) are continuous, so are the displacements u_r and u_φ in Eq. (6).

If the medium contains *liquid* layers, e.g. in cases where wave propagation through the ocean or the earth's core is to be modelled, the displacement vector

is irrotational, $\mathbf{u} = \text{grad}\, \phi$, and the boundary conditions are in principle different from those given above. However, computational experience shows that liquid layers are modelled perfectly by solid layers whose S velocity is of the order of 0.001 times the P velocity. Thus, algorithms for solid media are sufficient for all practical purposes.

The continuity of the quantities in Eq. (8a and b) at interfaces implies that interaction takes place between P waves, derived from ϕ, and S waves, derived from ψ. The S waves, represented by u_y and polarized horizontally, propagate independently. The S waves derived from ψ are called SV waves and those derived from u_y, SH waves. Similar conclusions follow from (9a and b): Ψ is the potential of the SV waves, and χ the potential of the SH waves. Note that, according to Eq. (6), SV waves contribute also to the horizontal transverse component u_φ and SH waves to the horizontal radial component u_r. Both contributions are, however, near-field terms for point sources. In the far-field of point sources, SV waves are polarized in rz-planes and SH waves, perpendicular to rz-planes.

3. Plane waves in layered media

3.1. Reflection and transmission at an interface

Here we consider the case of one interface, separating two homogeneous half-spaces, and determine the reflection and transmission coefficients of this interface for plane harmonic waves. These coefficients are essential quantities for the treatment of layered media, as will become clear in Section 3.2, but they are also of general interest to seismologists because they can sometimes be used for simple estimates of body-wave amplitudes. We use Cartesian coordinates and the corresponding displacement components, equations and boundary conditions compiled above. The interface is at $z = 0$.

The two cases sketched in Fig. 1 have to be treated, that of a *downgoing* incident wave (case I) and that of an *upgoing* incident wave (case II). In case I the incident wave travels in half-space 1, in case II in half-space 2. We consider case I in more detail.

If the incident wave is a P wave, the secondary waves produced at the interface are of P and SV type. Then we assume the following expressions for the displacement potentials in both half-spaces ($j = $ imaginary unit):

$$\phi_1 = e^{j(\omega t - kx - l_1 z)} \quad \text{(incident } P \text{ wave),}$$
$$+ R_{pp}^d\, e^{j(\omega t - kx + l_1 z)} \quad \text{(reflected } P \text{ wave)}$$
$$\psi_1 = R_{ps}^d\, e^{j(\omega t - kx + l_1' z)} \quad \text{(reflected } SV \text{ wave),} \qquad (10)$$
$$\phi_2 = T_{pp}^d\, e^{j(\omega t - kx - l_2 z)} \quad \text{(transmitted } P \text{ wave),}$$
$$\psi_2 = T_{ps}^d\, e^{j(\omega t - kx - l_2' z)} \quad \text{(transmitted } SV \text{ wave).}$$

The incident P wave has unit potential amplitude. Then, the amplitudes of the secondary waves are identical with the reflection and transmission coefficients for *potential* amplitudes. These coefficients have a superscript d, indicating that they correspond to a downgoing incident wave. All terms in Eq. (10) have plane-wave form and satisfy the wave equations (4). All waves travel horizontally with the same horizontal wavenum-
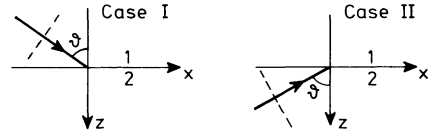

Fig. 1. Incidence of a plane wave at the interface $z = 0$ between two half-spaces 1 and 2. ϑ is the angle of incidence

ber k, in fulfilment of Snell's law. The relation between k and the angle of incidence ϑ (Fig. 1) is

$$k = \frac{\omega}{\alpha_1} \sin \vartheta. \qquad (11)$$

The vertical wavenumbers $l_{1,2}$ and $l'_{1,2}$ are

$$l_{1,2} = \left(\frac{\omega^2}{\alpha_{1,2}^2} - k^2 \right)^{1/2}, \qquad l'_{1,2} = \left(\frac{\omega^2}{\beta_{1,2}^2} - k^2 \right)^{1/2}, \qquad (12)$$

and the signs in front of them in Eq. (10) are negative (positive) for propagation in positive (negative) z-direction.

The boundary conditions for $z = 0$ can be formulated with the ϕ- and ψ-dependent quantities in Eq. (8a and b) and with Eq. (10). For instance, continuity of the horizontal displacement u_x yields:

$$\phi_{1,x} - \psi_{1,z} = \phi_{2,x} - \psi_{2,z} \quad (z = 0).$$

The following four equations for the reflection and transmission coefficients are obtained in matrix form:

$$
\begin{pmatrix}
-k & -l_1' & k & -l_2' \\
l_1 & -k & l_2 & k \\
\rho_1 \omega^2 - 2\mu_1 k^2 & -2\mu_1 k l_1' & 2\mu_2 k^2 - \rho_2 \omega^2 & -2\mu_2 k l_2' \\
2\mu_1 k l_1 & \rho_1 \omega^2 - 2\mu_1 k^2 & 2\mu_2 k l_2 & 2\mu_2 k^2 - \rho_2 \omega^2
\end{pmatrix}
$$
$$
\cdot \begin{pmatrix} R_{pp}^d \\ R_{ps}^d \\ T_{pp}^d \\ T_{ps}^d \end{pmatrix} = \begin{pmatrix} k \\ l_1 \\ 2\mu_1 k^2 - \rho_1 \omega^2 \\ 2\mu_1 k l_1 \end{pmatrix} \qquad (13)
$$

The apparent frequency dependence of these equations can be removed if the wavenumbers are replaced by *slownesses*:

$$u = \frac{k}{\omega} = \frac{\sin \vartheta}{\alpha_1} \quad \text{(horizontal slowness),} \qquad (14)$$

$$
\left.
\begin{aligned}
a_{1,2} &= \frac{l_{1,2}}{\omega} = (\alpha_{1,2}^{-2} - u^2)^{1/2} \\
b_{1,2} &= \frac{l'_{1,2}}{\omega} = (\beta_{1,2}^{-2} - u^2)^{1/2}
\end{aligned}
\right\} \quad \text{(vertical slownesses).} \qquad (15)
$$

Then, Eq. (13) tranforms into the equation

$$
\begin{pmatrix}
-u & -b_1 & u & -b_2 \\
a_1 & -u & a_2 & u \\
\rho_1 - 2\mu_1 u^2 & -2\mu_1 u b_1 & 2\mu_2 u^2 - \rho_2 & -2\mu_2 u b_2 \\
2\mu_1 u a_1 & \rho_1 - 2\mu_1 u^2 & 2\mu_2 u a_2 & 2\mu_2 u^2 - \rho_2
\end{pmatrix}
$$
$$
\cdot \begin{pmatrix} R_{pp}^d \\ R_{ps}^d \\ T_{pp}^d \\ T_{ps}^d \end{pmatrix} = \begin{pmatrix} u \\ a_1 \\ 2\mu_1 u^2 - \rho_1 \\ 2\mu_1 u a_1 \end{pmatrix}. \qquad (16)
$$

Table 1. Plane-wave reflection and transmission coefficients of a plane interface between two half-spaces (P velocities $\alpha_{1,2}$, S velocities $\beta_{1,2}$, densities $\rho_{1,2}$, horizontal slowness u). R^d and T^d are coefficients for *potential* amplitudes of $P-SV$ waves, r^d and t^d coefficients for *displacement* amplitudes of SH waves. The incident wave travels in the medium with index 1 (downward propagation, case I of Fig. 1)

R^d_{pp}	$\dfrac{D^d_2 - D^d_1}{D^d_1 + D^d_2}$
R^d_{ps}	$-\dfrac{2u a_1}{D^d_1 + D^d_2}\{(cu^2 - \rho_1 + \rho_2)(cu^2 + \rho_2) + c(cu^2 - \rho_1)a_2 b_2\}$
T^d_{pp}	$\dfrac{2\rho_1 a_1}{D^d_1 + D^d_2}\{(cu^2 + \rho_2)b_1 - (cu^2 - \rho_1)b_2\}$
T^d_{ps}	$-\dfrac{2\rho_1 u a_1}{D^d_1 + D^d_2}\{cu^2 - \rho_1 + \rho_2 + c a_2 b_1\}$
R^d_{ss}	$\dfrac{D^d_2 - D^d_1 - 2\rho_1 \rho_2(a_1 b_2 - a_2 b_1)}{D^d_1 + D^d_2}$
R^d_{sp}	$\dfrac{2u b_1}{D^d_1 + D^d_2}\{(cu^2 - \rho_1 + \rho_2)(cu^2 + \rho_2) + c(cu^2 - \rho_1)a_2 b_2\}$
T^d_{ss}	$\dfrac{2\rho_1 b_1}{D^d_1 + D^d_2}\{(cu^2 + \rho_2)a_1 - (cu^2 - \rho_1)a_2\}$
T^d_{sp}	$\dfrac{2\rho_1 u b_1}{D^d_1 + D^d_2}\{cu^2 - \rho_1 + \rho_2 + c a_1 b_2\}$
r^d	$\dfrac{\mu_1 b_1 - \mu_2 b_2}{\mu_1 b_1 + \mu_2 b_2}$
t^d	$\dfrac{2\mu_1 b_1}{\mu_1 b_1 + \mu_2 b_2}$

$$D^d_1 = (cu^2 - \rho_1 + \rho_2)^2 u^2 + (cu^2 - \rho_1)^2 a_2 b_2 + \rho_1 \rho_2 a_2 b_1$$
$$D^d_2 = c^2 u^2 a_1 a_2 b_1 b_2 + (cu^2 + \rho_2)^2 a_1 b_1 + \rho_1 \rho_2 a_1 b_2$$

$a_{1,2} = (\alpha_{1,2}^{-2} - u^2)^{1/2}$ positive real or
$b_{1,2} = (\beta_{1,2}^{-2} - u^2)^{1/2}$ negative imaginary for $\omega > 0$ or positive imaginary for $\omega < 0$

$c = 2(\mu_1 - \mu_2)$, $\mu_{1,2} = \rho_{1,2}\beta_{1,2}^2$

Application of Cramer's rule to this equation is cumbersome but rewarding, since relatively compact expressions for the reflection and transmission coefficients result. They are given in Table 1.

The case of an incident SV wave can be treated along the same lines, starting with the appropriate potentials instead of Eq. (10). The reflection and transmission coefficients follow from the equation

$$\begin{pmatrix} -u & -b_1 & u & -b_2 \\ a_1 & -u & a_2 & u \\ \rho_1 - 2\mu_1 u^2 & -2\mu_1 u b_1 & 2\mu_2 u^2 - \rho_2 & -2\mu_2 u b_2 \\ 2\mu_1 u a_1 & \rho_1 - 2\mu_1 u^2 & 2\mu_2 u a_2 & 2\mu_2 u^2 - \rho_2 \end{pmatrix}$$

$$\cdot \begin{pmatrix} R^d_{sp} \\ R^d_{ss} \\ T^d_{sp} \\ T^d_{ss} \end{pmatrix} = \begin{pmatrix} -b_1 \\ u \\ -2\mu_1 u b_1 \\ 2\mu_1 u^2 - \rho_1 \end{pmatrix} \qquad (17)$$

and are included in Table 1.

The case of an incident SH wave is much simpler than the $P-SV$ case, since there is no conversion to P or SV waves at the interface. The displacements are:

$$u_{y1} = e^{j(\omega t - kx - l'_1 z)} \qquad \text{(incident } SH \text{ wave)},$$
$$+ r^d e^{j(\omega t - kx + l'_1 z)} \qquad \text{(reflected } SH \text{ wave)}, \qquad (18)$$
$$u_{y2} = t^d e^{j(\omega t - kx - l'_2 z)} \qquad \text{(transmitted } SH \text{ wave)}.$$

The reflection and transmission coefficients, which here are coefficients for *displacement* amplitudes, follow from the continuity conditions for u_y and $\mu u_{y,z}$ at $z = 0$ [see Eq. (8a and b)]. They are also given in Table 1.

$P-SV$ reflection and transmission coefficients for *displacement* amplitudes follow from the potential coefficients in Table 1 by multiplication with factors which are quotients of the velocity of the incident wave and the velocity of the secondary wave.

The coefficients in Table 1 depend only on the velocities and densities of the two half-spaces and on slowness or angle of incidence, according to Eq. (14). They can become complex, if one or more of the vertical slownesses $a_{1,2}$ and $b_{1,2}$ are imaginary. In this case some of the secondary waves are inhomogeneous waves which propagate horizontally and whose amplitudes decay exponentially with increasing vertical distance from the interface; this follows from Eqs. (10) or (18). In this case there is a slight frequency-dependence of the reflection and transmission coefficients according to the sign of ω, as indicated in Table 1. For numerical calculations it is usually sufficient to consider $\omega \geq 0$; then the reflection and transmission coefficients of an interface are *frequency-independent*.

The reflection and transmission coefficients in case II of Fig. 1, i.e. for incidence at the interface $z = 0$ from below, follow from those in Table 1 by two changes. The first is an interchange of the parameters of both media, the second a sign change for those $P-SV$ coefficients which imply wave conversion at the interface. This sign change is a consequence of the change, with respect to case I, in propagation directions relative to the z-axis. The coefficients are summarized in Table 2; their superscript u indicates that the incident wave is upgoing.

The coefficients in Tables 1 and 2 are the essential basis for the calculation of reflection and transmission coefficients of *layered* media with an arbitrary number of interfaces. The recursive calculation of these reflectivities and transmissivities will be described in the next section.

3.2 Reflection and transmission at a layer stack

We consider a stack of $n-1$ layers between two homogeneous half-spaces. The upper half-space has the index 0, the half-space at the bottom the index n, the parameters of the medium i are α_i, β_i, ρ_i and the thickness d_i, and the layers i and $i+1$ are separated by the interface $z = z_{i+1}$. We treat the case of incident waves travelling downwards in the upper half-space in some detail. The results for the case of incident waves, travelling upwards in the lower half-space, are summarized in Section 3.2.3.

Table 2. Plane-wave reflection and transmission coefficients as in Table 1, but for an incident wave travelling in the medium with index 2 (upward propagation, case II of Fig. 1)

R_{pp}^u	$\dfrac{D_2^u - D_1^u}{D_1^u + D_2^u}$
R_{ps}^u	$\dfrac{2u\,a_2}{D_1^u + D_2^u}\{(cu^2 - \rho_1 + \rho_2)(cu^2 - \rho_1) + c(cu^2 + \rho_2)a_1 b_1\}$
T_{pp}^u	$\dfrac{2\rho_2\,a_2}{D_1^u + D_2^u}\{(cu^2 + \rho_2)b_1 - (cu^2 - \rho_1)b_2\}$
T_{ps}^u	$-\dfrac{2\rho_2\,u\,a_2}{D_1^u + D_2^u}\{cu^2 - \rho_1 + \rho_2 + ca_1 b_2\}$
R_{ss}^u	$\dfrac{D_2^u - D_1^u - 2\rho_1\rho_2(a_2 b_1 - a_1 b_2)}{D_1^u + D_2^u}$
R_{sp}^u	$-\dfrac{2u\,b_2}{D_1^u + D_2^u}\{(cu^2 - \rho_1 + \rho_2)(cu^2 - \rho_1) + c(cu^2 + \rho_2)a_1 b_1\}$
T_{ss}^u	$\dfrac{2\rho_2\,b_2}{D_1^u + D_2^u}\{(cu^2 + \rho_2)a_1 - (cu^2 - \rho_1)a_2\}$
T_{sp}^u	$\dfrac{2\rho_2\,u\,b_2}{D_1^u + D_2^u}\{cu^2 - \rho_1 + \rho_2 + ca_2 b_1\}$
r^u	$\dfrac{\mu_2 b_2 - \mu_1 b_1}{\mu_1 b_1 + \mu_2 b_2}$
t^u	$\dfrac{2\mu_2 b_2}{\mu_1 b_1 + \mu_2 b_2}$

$D_1^u = (cu^2 - \rho_1 + \rho_2)^2 u^2 + (cu^2 + \rho_2)^2 a_1 b_1 + \rho_1\rho_2 a_1 b_2$

$D_2^u = c^2 u^2 a_1 a_2 b_1 b_2 + (cu^2 - \rho_1)^2 a_2 b_2 + \rho_1\rho_2 a_2 b_1$

Other quantities as in Table 1

3.2.1 P − SV case.

In the $P-SV$ case the displacement potentials in layer i are, in analogy to Eq. (10):

$$\left.\begin{aligned}\phi_i &= e^{-jkx}\left[A_i e^{-jl_i(z-z_i)} + B_i e^{+jl_i(z-z_i)}\right]\\ \psi_i &= e^{-jkx}\left[C_i e^{-jl_i'(z-z_i)} + D_i e^{+jl_i'(z-z_i)}\right]\end{aligned}\right\}\quad i = 0, 1, \ldots, n. \tag{19}$$

The time factor $e^{j\omega t}$ has been suppressed. The first terms in Eq. (19) represent all downgoing waves in layer i, the second terms all upgoing waves. Then we define *reflectivities* at the top of layer i by the amplitude ratios of upgoing and downgoing waves:

$$PPT_i = \frac{B_i}{A_i}, \quad PST_i = \frac{D_i}{A_i},$$

$$SPT_i = \frac{B_i}{C_i}, \quad SST_i = \frac{D_i}{C_i}.$$

The first letter of each reflectivity denotes the type of the incident wave, the second letter denotes the type of the secondary wave and T stands for top. We combine the reflectivities in the *local reflectivity matrix*

$$\mathbf{MT}_i = \begin{pmatrix} PPT_i & SPT_i \\ PST_i & SST_i \end{pmatrix}. \tag{20}$$

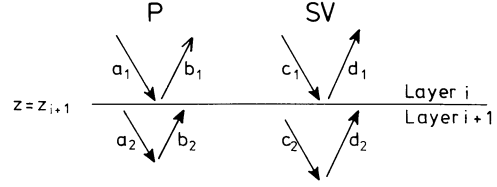Similarly, we have for the bottom of layer i:

Fig. 2. Potential amplitudes of downgoing and upgoing waves immediately above and below the interface $z = z_{i+1}$

$$PPB_i = \frac{B_i e^{+jl_i d_i}}{A_i e^{-jl_i d_i}} = PPT_i e^{+2jl_i d_i},$$

$$PSB_i = \frac{D_i e^{+jl_i' d_i}}{A_i e^{-jl_i d_i}} = PST_i e^{+j(l_i' + l_i)d_i}, \quad \text{etc.}$$

$$\mathbf{MB_i} = \begin{pmatrix} PPB_i & SPB_i \\ PSB_i & SSB_i \end{pmatrix}. \tag{21}$$

The relation between the reflectivity matrices at the top and the bottom of layer i is

$$\mathbf{MT_i} = \mathbf{E_i}\,\mathbf{MB_i}\,\mathbf{E_i} \tag{22}$$

with the *phase matrix*

$$\mathbf{E_i} = \begin{pmatrix} e^{-jl_i d_i} & 0 \\ 0 & e^{-jl_i' d_i} \end{pmatrix}. \tag{23}$$

The relation between the reflectivity matrices at the bottom of layer i, $\mathbf{MB_i}$, and at the top of layer $i+1$, $\mathbf{MT_{i+1}}$, is more complicated; here the reflection and transmission coefficients of the interface $z = z_{i+1}$ come into play. We abbreviate the potential amplitudes of downgoing and upgoing waves at the bottom of layer i, i.e. immediately above the interface, by a_1, b_1, c_1, d_1 (Fig. 2); similarly a_2, b_2, c_2, d_2 define the amplitudes immediately below the interface (there should be no confusion with slownesses and layer thicknesses). The relation between these amplitudes is:

$$\begin{aligned} a_2 &= T_{pp}^d a_1 + R_{pp}^u b_2 + T_{sp}^d c_1 + R_{sp}^u d_2 \\ c_2 &= T_{ps}^d a_1 + R_{ps}^u b_2 + T_{ss}^d c_1 + R_{ss}^u d_2 \\ b_1 &= R_{pp}^d a_1 + T_{pp}^u b_2 + R_{sp}^d c_1 + T_{sp}^u d_2 \\ d_1 &= R_{ps}^d a_1 + T_{ps}^u b_2 + R_{ss}^d c_1 + T_{ss}^u d_2 \ . \end{aligned} \tag{24}$$

The coefficients $R^{d,u}$ and $T^{d,u}$ are the plane-wave reflection and transmission coefficients of the interface $z = z_{i+1}$; they follow from Tables 1 and 2 by replacing the parameters $\alpha_1, \beta_1, \rho_1$ there by $\alpha_i, \beta_i, \rho_i$ and $\alpha_2, \beta_2, \rho_2$ by $\alpha_{i+1}, \beta_{i+1}, \rho_{i+1}$. The left sides of Eq. (24) are the amplitudes of the four waves travelling away from the interface; they are linear combinations of the amplitudes of all four incident waves, the weights being the appropriate reflection and transmission coefficients. We combine these coefficients into *matrices of interface reflection and transmission coefficients*

$$\mathbf{R_{i+1}^{d,u}} = \begin{pmatrix} R_{pp}^{d,u} & R_{sp}^{d,u} \\ R_{ps}^{d,u} & R_{ss}^{d,u} \end{pmatrix},$$

$$\mathbf{T_{i+1}^{d,u}} = \begin{pmatrix} T_{pp}^{d,u} & T_{sp}^{d,u} \\ T_{ps}^{d,u} & T_{ss}^{d,u} \end{pmatrix}, \tag{25}$$

and replace Eq. (24) by two vector equations:

$$\begin{pmatrix} a_2 \\ c_2 \end{pmatrix} = \mathbf{T_{i+1}^d} \begin{pmatrix} a_1 \\ c_1 \end{pmatrix} + \mathbf{R_{i+1}^u} \begin{pmatrix} b_2 \\ d_2 \end{pmatrix} \tag{26}$$

$$\begin{pmatrix} b_1 \\ d_1 \end{pmatrix} = \mathbf{R_{i+1}^d} \begin{pmatrix} a_1 \\ c_1 \end{pmatrix} + \mathbf{T_{i+1}^u} \begin{pmatrix} b_2 \\ d_2 \end{pmatrix}. \tag{27}$$

The amplitudes b_1, d_1, b_2, d_2 of the upgoing waves can also be expressed with the aid of the reflectivities at the bottom of layer i and at the top of layer $i+1$:

$$\left.\begin{array}{l} b_1 = a_1 PPB_i + c_1 SPB_i \\ d_1 = a_1 PSB_i + c_1 SSB_i \end{array}\right\} \quad \begin{pmatrix} b_1 \\ d_1 \end{pmatrix} = \mathbf{MB_i} \begin{pmatrix} a_1 \\ c_1 \end{pmatrix} \tag{28}$$

$$\left.\begin{array}{l} b_2 = a_2 PPT_{i+1} + c_2 SPT_{i+1} \\ d_2 = a_2 PST_{i+1} + c_2 SST_{i+1} \end{array}\right\} \quad \begin{pmatrix} b_2 \\ d_2 \end{pmatrix} = \mathbf{MT_{i+1}} \begin{pmatrix} a_2 \\ c_2 \end{pmatrix}. \tag{29}$$

Equation (26) is inserted into Eq. (29):

$$\begin{pmatrix} b_2 \\ d_2 \end{pmatrix} = \mathbf{MT_{i+1}} \left[\mathbf{T_{i+1}^d} \begin{pmatrix} a_1 \\ c_1 \end{pmatrix} + \mathbf{R_{i+1}^u} \begin{pmatrix} b_2 \\ d_2 \end{pmatrix} \right].$$

The solution of this equation is

$$\begin{pmatrix} b_2 \\ d_2 \end{pmatrix} = [\mathbf{I} - \mathbf{MT_{i+1}} \mathbf{R_{i+1}^u}]^{-1} \mathbf{MT_{i+1}} \mathbf{T_{i+1}^d} \begin{pmatrix} a_1 \\ c_1 \end{pmatrix} \tag{30}$$

where $\mathbf{I}$ is the 2×2 identity matrix. From Eqs. (27) and (28) one obtains

$$\mathbf{MB_i} \begin{pmatrix} a_1 \\ c_1 \end{pmatrix} = \mathbf{R_{i+1}^d} \begin{pmatrix} a_1 \\ c_1 \end{pmatrix} + \mathbf{T_{i+1}^u} \begin{pmatrix} b_2 \\ d_2 \end{pmatrix}.$$

Inserting Eq. (30) here, we find the desired relation between $\mathbf{MB_i}$ and $\mathbf{MT_{i+1}}$:

$$\mathbf{MB_i} = \mathbf{R_{i+1}^d} + \mathbf{T_{i+1}^u} [\mathbf{I} - \mathbf{MT_{i+1}} \mathbf{R_{i+1}^u}]^{-1} \mathbf{MT_{i+1}} \mathbf{T_{i+1}^d}. \tag{31}$$

Equations (31) and (22) together relate the reflectivity matrices at the top of layers $i+1$ and i.

Our final aim is to calculate the *overall reflectivity matrix*

$$\mathbf{RR^d} = \begin{pmatrix} RR_{pp}^d & RR_{sp}^d \\ RR_{ps}^d & RR_{ss}^d \end{pmatrix} = \mathbf{MB_0} \tag{32}$$

at the bottom of the upper half-space, since the elements of this matrix are just the desired reflection coefficients or reflectivities of the medium (for potential amplitudes). Therefore, we apply Eqs. (31) and (22) *recursively*. We start with $i = n-1$ and $\mathbf{MT_n} = \mathbf{0}$, which is the logical condition for any level inside the lower half-space. Then, the reflectivity matrix at the bottom of layer $n-1$ is just the matrix of reflection coefficients of the interface $z = z_n$ for downgoing incident waves: $\mathbf{MB_{n-1}} = \mathbf{R_n^d}$. By successive applications of Eqs. (22) and (31) one moves upwards through the medium, until $i = 0$ is reached. The reflectivity matrix becomes increasingly more complicated, since it now also represents multiples and conversions produced at the interfaces.

For practical purposes it may be useful to relate the reflectivity matrix to a level *inside* the upper half-space;

this is achieved by another application of Eq. (22) and introduces only phase shifts.

The great advantage of the recursive algorithm described is that it is unconditionally stable for all frequencies and slownesses. Other methods sometimes suffer from overflow problems in the calculation of exponential functions for high frequencies and slownesses (see e.g., Kennett, 1983, Sec. 6.2.2). Here, exponential functions appear only in the phase matrix (23), and the sign of their arguments guarantees that they are always bounded.

The *transmission properties* of the layered medium for incident waves coming from above can be found in a similar way to the reflection properties. We define transmissivities at the top of layer i by comparing the amplitudes of the downgoing waves there and in the upper half-space [see Eq. (19)]:

$$\overline{PPT_i} = \frac{A_i}{A_0}, \qquad \overline{PST_i} = \frac{C_i}{A_0},$$

$$\overline{SPT_i} = \frac{A_i}{C_0}, \qquad \overline{SST_i} = \frac{C_i}{C_0}.$$

We combine them into a *local transmissivity matrix*

$$\overline{\mathbf{MT_i}} = \begin{pmatrix} \overline{PPT_i} & \overline{SPT_i} \\ \overline{PST_i} & \overline{SST_i} \end{pmatrix}.$$

Similarly we have for the bottom of layer i:

$$\overline{PPB_i} = \frac{A_i e^{-jl_i d_i}}{A_0} = \overline{PPT_i} e^{-jl_i d_i}, \text{ etc.}$$

$$\overline{\mathbf{MB_i}} = \begin{pmatrix} \overline{PPB_i} & \overline{SPB_i} \\ \overline{PSP_i} & \overline{SSB_i} \end{pmatrix} = \mathbf{E_i} \overline{\mathbf{MT_i}} \tag{33}$$

with the phase matrix $\mathbf{E_i}$ from Eq. (23).

The relation between $\overline{\mathbf{MB_i}}$ and $\overline{\mathbf{MT_{i+1}}}$ follows from a consideration of the interface $z = z_{i+1}$, similar to that above (Fig. 2). We have:

$$\begin{pmatrix} a_1 \\ c_1 \end{pmatrix} = \overline{\mathbf{MB_i}} \begin{pmatrix} A_0 \\ C_0 \end{pmatrix} \tag{34}$$

$$\begin{pmatrix} a_2 \\ c_2 \end{pmatrix} = \overline{\mathbf{MT_{i+1}}} \begin{pmatrix} A_0 \\ C_0 \end{pmatrix}. \tag{35}$$

On the other hand, from Eqs. (26) and (29):

$$\begin{pmatrix} a_2 \\ c_2 \end{pmatrix} = \mathbf{T_{i+1}^d} \begin{pmatrix} a_1 \\ c_1 \end{pmatrix} + \mathbf{R_{i+1}^u} \begin{pmatrix} b_2 \\ d_2 \end{pmatrix}$$

$$= \mathbf{T_{i+1}^d} \begin{pmatrix} a_1 \\ c_1 \end{pmatrix} + \mathbf{R_{i+1}^u} \mathbf{MT_{i+1}} \begin{pmatrix} a_2 \\ c_2 \end{pmatrix}.$$

Hence:

$$\begin{pmatrix} a_2 \\ c_2 \end{pmatrix} = [\mathbf{I} - \mathbf{R_{i+1}^u} \mathbf{MT_{i+1}}]^{-1} \mathbf{T_{i+1}^d} \begin{pmatrix} a_1 \\ c_1 \end{pmatrix}.$$

Inserting Eqs. (34) and (35), we obtain

$$\overline{\mathbf{MT_{i+1}}} = [\mathbf{I} - \mathbf{R_{i+1}^u} \mathbf{MT_{i+1}}]^{-1} \mathbf{T_{i+1}^d} \overline{\mathbf{MB_i}}. \tag{36}$$

The recursion, based on Eqs. (36) and (33), starts with $i = 0$ and $\overline{\mathbf{MB_0}} = \mathbf{I}$. The *overall transmissivity matrix* is

$$\mathbf{TT^d} = \begin{pmatrix} TT_{pp}^d & TT_{sp}^d \\ TT_{ps}^d & TT_{ss}^d \end{pmatrix} = \overline{\mathbf{MT_n}} \tag{37}$$

and has as its elements the transmission coefficients or transmissivities of the medium (again for potential amplitudes).

It is, however, not advisable to perform the recursion in this form in practice because it would require that the reflectivity matrices $\mathbf{MT_{i+1}}$ be calculated and stored *prior* to the calculation of $\mathbf{TT^d}$. Rather, one uses the form

$$\mathbf{TT^d} = \mathbf{F_{n-1}} \, \mathbf{F_{n-2}} \dots \mathbf{F_0}, \tag{38}$$

where

$$\mathbf{F_i} = [\mathbf{I} - \mathbf{R_{i+1}^u} \, \mathbf{MT_{i+1}}]^{-1} \, \mathbf{T_{i+1}^d} \, \mathbf{E_i} \tag{39}$$

$(\mathbf{E_0} = \mathbf{I}, \ \mathbf{MT_n} = \mathbf{0})$. If the matrix multiplication in Eq. (38) is performed from left to right, the calculation of $\mathbf{TT^d}$ can directly be combined with the calculation of the reflectivity matrix $\mathbf{RR^d}$.

$\mathbf{TT^d}$ is the transmissivity of the depth range between the uppermost and the lowermost interface of the medium. If it is desirable also to include parts of the half-spaces, Eq. (38) can also be used with additional phase matrices (23) multiplied from right and left.

3.2.2 SH case. In this section we give only the results for the *scalar* reflectivity RR^d and the *scalar* transmissivity TT^d, which here express the displacement-amplitude ratio of the secondary (reflected or transmitted) and the incident SH wave. As in the $P-SV$ case, RR^d refers to the interface $z = z_1$ between the upper half-space and the first layer, and TT^d to the lowermost interface $z = z_n$. It is clear that the principles of the derivation of RR^d and TT^d are the same as in the $P-SV$ case, but the derivation itself is much simpler; it is actually a good exercise for the interested reader. One obtains:

$$RR^d = MB_0 \tag{40}$$

$$\left. \begin{array}{l} MB_i = r_{i+1}^d + \dfrac{t_{i+1}^d \, t_{i+1}^u \, MT_{i+1}}{1 - r_{i+1}^u \, MT_{i+1}} \\[3mm] MT_i = MB_i \, e^{-2jl_i'd_i} \end{array} \right\} \ i = n-1, \ n-2, \dots, 0 \tag{41}$$

$$TT^d = \prod_{i=0}^{n-1} F_i \tag{42}$$

$$F_i = \frac{t_{i+1}^d \, e^{-jl_i'd_i}}{1 - r_{i+1}^u \, MT_{i+1}}. \tag{43}$$

In Eq. (41) one uses $MT_n = 0$, and the factor F_0 in Eq. (43) is obtained by setting $d_0 = 0$. The interface coefficients $r^{d,u}$ and $t^{d,u}$ follow from Tables 1 and 2. Comparison of the SH results with those for the $P-SV$ case, e.g. of Eq. (41) and Eqs. (31) plus (22), shows the great similarity in basic structure.

3.2.3 Wave incidence from below. The layered medium is the same as before, but now the incident waves travel upwards in the lower half-space. In this case the overall reflectivity matrix $\mathbf{RR^u}$ expresses, for a level at the top of the lower half-space, the potential-amplitude ratios of downgoing reflected and upgoing incident waves. The overall transmissivity matrix $\mathbf{TT^u}$ relates the amplitudes of upgoing transmitted waves at the bottom of the upper half-space and the amplitudes of the upgoing incident waves at the top of the lower half-space. Similar definitions hold for the scalar SH reflectivity RR^u and transmissivity TT^u.

The recursion, leading to $\mathbf{RR^u}$, is as follows:

$$\left. \begin{array}{l} \mathbf{NB_0} = \mathbf{0} \\[1mm] \mathbf{NT_{i+1}} = \mathbf{R_{i+1}^u} + \mathbf{T_{i+1}^d} \\[1mm] \cdot [\mathbf{I} - \mathbf{NB_i} \, \mathbf{R_{i+1}^d}]^{-1} \, \mathbf{NB_i} \, \mathbf{T_{i+1}^u} \\[1mm] \mathbf{NB_{i+1}} = \mathbf{E_{i+1}} \, \mathbf{NT_{i+1}} \, \mathbf{E_{i+1}} \end{array} \right\} \ i = 0, 1, \dots, n-1 \tag{44}$$

$$\mathbf{RR^u} = \begin{pmatrix} RR_{pp}^u & RR_{sp}^u \\ RR_{ps}^u & RR_{ss}^u \end{pmatrix} = \mathbf{NT_n}. \tag{45}$$

The local reflectivity matrices $\mathbf{NT_i}$ and $\mathbf{NB_i}$ correspond to the top and the bottom of layer i, respectively. They are different from the matrices $\mathbf{MT_i}$ and $\mathbf{MB_i}$ in Section 3.2.1, because they relate downgoing reflected and upgoing incident waves, whereas $\mathbf{MT_i}$ and $\mathbf{MB_i}$ relate upgoing reflected and downgoing incident waves.

The overall transmissivity matrix $\mathbf{TT^u}$ is:

$$\mathbf{TT^u} = \begin{pmatrix} TT_{pp}^u & TT_{sp}^u \\ TT_{ps}^u & TT_{ss}^u \end{pmatrix} = \mathbf{G_0} \, \mathbf{G_1} \dots \mathbf{G_{n-1}} \tag{46}$$

$$\mathbf{G_i} = \mathbf{E_i} [\mathbf{I} - \mathbf{R_{i+1}^d} \, \mathbf{NB_i}]^{-1} \, \mathbf{T_{i+1}^u}, \qquad \mathbf{G_0} = \mathbf{T_1^u}. \tag{47}$$

The matrix multiplication in Eq. (46) is performed from left to right, since the calculation of $\mathbf{TT^u}$ can then be directly combined with that of $\mathbf{RR^u}$.

The results for SH waves are:

$$\left. \begin{array}{l} NB_0 = 0 \\[2mm] NT_{i+1} = r_{i+1}^u + \dfrac{t_{i+1}^d \, t_{i+1}^u \, NB_i}{1 - r_{i+1}^d \, NB_i} \\[3mm] NB_{i+1} = NT_{i+1} \, e^{-2jl_{i+1}'d_{i+1}} \end{array} \right\} \ i = 0, 1, \dots, n-1 \tag{48}$$

$$RR^u = NT_n \tag{49}$$

$$TT^u = \prod_{i=0}^{n-1} G_i \tag{50}$$

$$G_i = \frac{t_{i+1}^u \, e^{-jl_i'd_i}}{1 - r_{i+1}^d \, NB_i}, \qquad G_0 = t_1^u. \tag{51}$$

4. Waves from point sources in layered media

4.1 Elementary displacement potentials for cylindrical coordinates

Elementary solutions of the wave equations (7) for the $P-SV$ potentials in layer i of the medium, which will be used later for the synthesis of point-source wave fields, are the following:

$$\phi_i = \begin{Bmatrix} \cos l\varphi \\ \sin l\varphi \end{Bmatrix} J_l(kr)\left[A_i e^{-jl_i(z-z_i)} + B_i e^{+jl_i(z-z_i)}\right]$$

$$\Psi_i = \begin{Bmatrix} \cos l\varphi \\ \sin l\varphi \end{Bmatrix} J_l(kr)\frac{1}{jk}\left[C_i e^{-jl'_i(z-z_i)} + D_i e^{+jl'_i(z-z_i)}\right] \qquad\Bigg\} \; i = 0,1,\dots,n. \tag{52}$$

$J_l(kr)$ is the Bessel function of integer order $l = 0, 1, 2, \dots,$ and the time factor $e^{j\omega t}$ has been omitted as in the corresponding plane-wave (Cartesian coordinate) expressions, Eq. (19).

In the SV potential Ψ_i the term $(jk)^{-1}$ has been factored out since the equations for the coefficients A_i, B_i, C_i, D_i, which follow from the boundary conditions at interfaces [see Eq. (9a and b)], then agree exactly with the equations for the coefficients in Eq. (19) which are based on the continuity of the quantities (8a and b). This has the important consequence that the plane-wave reflectivity and transmissivity matrices that have been derived in Section 3 can be used directly here. For instance, the amplitudes of the upgoing wave field at the uppermost interface $z = z_1$, B_0 and D_0, follow from the amplitudes of the downgoing wave field, A_0 and C_0, with the aid of the reflectivity matrix $\mathbf{RR^d}$ in Eq. (32):

$$\begin{pmatrix} B_0 \\ D_0 \end{pmatrix} = \mathbf{RR^d}\begin{pmatrix} A_0 \\ C_0 \end{pmatrix}. \tag{53}$$

Similarly, if the amplitudes of the upgoing wave field at the lowermost interface $z = z_n$, B_n and D_n, are given, B_0 and D_0 follow from

$$\begin{pmatrix} B_0 \\ D_0 \end{pmatrix} = \mathbf{TT^u}\begin{pmatrix} B_n \\ D_n \end{pmatrix}, \tag{54}$$

where $\mathbf{TT^u}$ is the transmissivity matrix in Eq. (46).

The elementary SH potential in layer i is

$$\chi_i = \begin{Bmatrix} \cos l\varphi \\ \sin l\varphi \end{Bmatrix} J_l(kr)$$
$$\cdot\left[E_i e^{-jl'_i(z-z_i)} + F_i e^{+jl'_i(z-z_i)}\right], \tag{55}$$

and the scalar reflectivity and transmissivity of the plane-wave case can also be used here:

$$F_0 = RR^d E_0 \tag{56}$$

with RR^d from Eqs. (40) and (41), or

$$F_0 = TT^u F_n \tag{57}$$

with TT^u according to Eqs. (50) and (51).

Up till now, reflectivities and transmissivities have been described for the *complete* layered medium. It is clear that they can also be defined for partitions of the medium by simply deleting those layers which are not of interest. The reflectivities and transmissivities in this form will be used later on.

4.2 Displacement potentials for a single force

We consider now the layered medium with a single-force point source at depth z_s in layer m (Fig. 3). The single force $\mathbf{F}$ is harmonic in time and has frequency-dependent components F_1, F_2, F_3. These components refer to a Cartesian coordinate system with, say, the x-axis pointing north, the y-axis pointing east and the z-axis pointing down. The displacement potentials of the single force have the following slowness-integral representations for an observer with cylindrical coordinates (r, φ, z) in an infinite medium whose material properties are those of layer m:

$$4\pi\rho_m\phi_s = \varepsilon_1 \int_0^\infty \text{sign}(z-z_s)\, u\, J_0(u\omega r)\, e^{-j\omega a_m|z-z_s|}du$$
$$+ \varepsilon_2 \int_0^\infty \frac{u^2}{ja_m} J_1(u\omega r)\, e^{-j\omega a_m|z-z_s|}du \tag{58}$$

$$4\pi\rho_m\Psi_s = \varepsilon_1 \int_0^\infty \frac{u}{j\omega b_m} J_0(u\omega r)\, e^{-j\omega b_m|z-z_s|}du$$
$$+ \varepsilon_2 \int_0^\infty \frac{\text{sign}(z-z_s)}{\omega} J_1(u\omega r)\, e^{-j\omega b_m|z-z_s|}du \tag{59}$$

$$4\pi\rho_m\chi_s = \eta \int_0^\infty \frac{-1}{\beta_m^2 j b_m} J_1(u\omega r)\, e^{-j\omega b_m|z-z_s|}du \tag{60}$$

$$a_m = (\alpha_m^{-2} - u^2)^{1/2} \quad \text{(positive real or}$$
$$b_m = (\beta_m^{-2} - u^2)^{1/2} \quad \text{negative imaginary),} \tag{61}$$

$$\varepsilon_1 = F_3, \qquad \varepsilon_2 = F_1\cos\varphi + F_2\sin\varphi,$$
$$\eta = -F_1\sin\varphi + F_2\cos\varphi. \tag{62}$$

These source-potential representations are very similar to the well-known Sommerfeld integral for an explosive point source. They have been taken from Müller (1969) and were corrected for a misprint in the second term of the original form of Eq. (58).
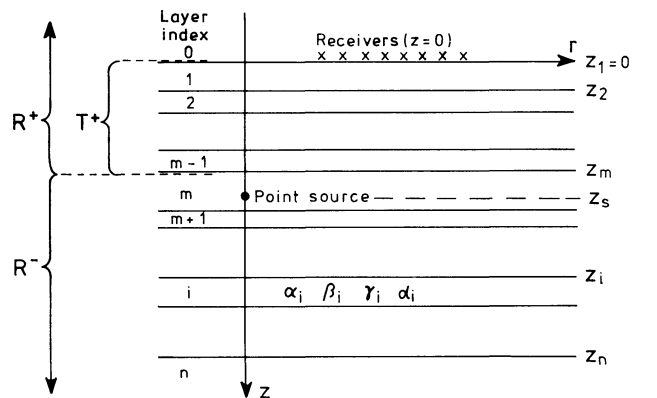
Fig. 3. Layered medium, consisting of $n-1$ homogeneous layers between two homogeneous half-spaces. Layer parameters are: $\alpha_i = P$ velocity, $\beta_i = S$ velocity, $\rho_i =$ density, $d_i =$ thickness, $z_i =$ depth to the top. *On the left* it is indicated to which partition of the medium the reflectivities $\mathbf{R}^\pm$, $R^\pm$ and the transmissivity $\mathbf{T^+}$, T^+ correspond

162

The integrands in Eqs. (58)–(60) have, in principle, the form of the elementary potentials (52) and (55) for $l = 0$ and $l = 1$ if the wavenumbers there are replaced by slownesses,

$$k = u\omega, \qquad l_i = a_i\omega, \qquad l'_i = b_i\omega,$$

with a_i and b_i defined in analogy to Eq. (61). Hence, it is clear that the interaction of the source wave field with the layer stacks above and below the source can also be represented by such slowness integrals. All that has to be done is to extract from Eqs. (58)–(60) *source amplitudes* $A_s, B_s, \ldots, F_s$ and then to describe the interaction by equations similar to Eqs. (53) and (54) or Eqs. (56) and (57).

The source amplitudes are different for downgoing and upgoing waves, and in the $P-SV$ case they are also different for the terms with different types of φ dependence. For downgoing waves ($z > z_s$) we obtain:

$$4\pi\rho_m \phi_s^d = \int_0^\infty (\varepsilon_1 A_{s1} J_0 + \varepsilon_2 A_{s2} J_1) e^{-j\omega a_m(z-z_m)} du \qquad (63)$$

$$4\pi\rho_m \Psi_s^d = \int_0^\infty \frac{1}{ju\omega} (\varepsilon_1 C_{s1} J_0 + \varepsilon_2 C_{s2} J_1) e^{-j\omega b_m(z-z_m)} du \qquad (64)$$

$$4\pi\rho_m \chi_s^d = \int_0^\infty \eta E_s J_1 e^{-j\omega b_m(z-z_m)} du \qquad (65)$$

$$A_{s1} = u e_\alpha, \qquad A_{s2} = \frac{u^2}{ja_m} e_\alpha,$$

$$C_{s1} = \frac{u^2}{b_m} e_\beta, \qquad C_{s2} = ju e_\beta, \qquad E_s = \frac{-1}{\beta_m^2 j b_m} e_\beta \qquad (66)$$

$$e_\alpha = e^{j\omega a_m(z_s - z_m)}, \qquad e_\beta = e^{j\omega b_m(z_s - z_m)}. \qquad (67)$$

Similar expressions hold for upgoing waves ($z < z_s$):

$$4\pi\rho_m \phi_s^u = \int_0^\infty (\varepsilon_1 B_{s1} J_0 + \varepsilon_2 B_{s2} J_1) e^{+j\omega a_m(z-z_m)} du \qquad (68)$$

$$4\pi\rho_m \Psi_s^u = \int_0^\infty \frac{1}{ju\omega} (\varepsilon_1 D_{s1} J_0 + \varepsilon_2 D_{s2} J_1) e^{+j\omega b_m(z-z_m)} du \qquad (69)$$

$$4\pi\rho_m \chi_s^u = \int_0^\infty \eta F_s J_1 e^{+j\omega b_m(z-z_m)} du \qquad (70)$$

$$B_{s1} = -u e_\alpha^{-1}, \qquad B_{s2} = \frac{u^2}{ja_m} e_\alpha^{-1}$$

$$D_{s1} = \frac{u^2}{b_m} e_\beta^{-1}, \qquad D_{s2} = -ju e_\beta^{-1}, \qquad (71)$$

$$F_s = \frac{-1}{\beta_m^2 j b_m} e_\beta^{-1}.$$

For later use, it is favourable to combine the $P-SV$ source amplitudes into *source amplitude vectors*:

$$\mathbf{S}_{1,2}^d = \begin{pmatrix} A_{s1,2} \\ C_{s1,2} \end{pmatrix}, \qquad \mathbf{S}_{1,2}^u = \begin{pmatrix} B_{s1,2} \\ D_{s1,2} \end{pmatrix}. \qquad (72)$$

Moreover, we write

$$S^d = E_s, \qquad S^u = F_s \qquad (73)$$

for the SH source amplitudes, in order to have unified notation.

4.3 Synthesis of the wave field at $z = 0$

The *first step* in the wave-field synthesis is to determine the complete upgoing wave field in layer m. This field is the sum of the direct upgoing waves, Eqs. (68), (69) and (70), and all possible reflections and multiple reflections at the layer stacks above and below the level $z = z_m$ (in the sense of z_m^+) in layer m. Each of these contributions, and also their sum, can be written in a form similar to Eq. (68), (69) or (70):

$$4\pi\rho_m \phi^u = \int_0^\infty (\varepsilon_1 B_1 J_0 + \varepsilon_2 B_2 J_1) e^{+j\omega a_m(z-z_m)} du$$

$$4\pi\rho_m \Psi^u = \int_0^\infty \frac{1}{ju\omega} (\varepsilon_1 D_1 J_0 + \varepsilon_2 D_2 J_1) e^{+j\omega b_m(z-z_m)} du \qquad (74)$$

$$4\pi\rho_m \chi^u = \int_0^\infty \eta V J_1 e^{+j\omega b_m(z-z_m)} du.$$

The contributions differ in the $P-SV$ *amplitude vectors*

$$\mathbf{V}_{1,2} = \begin{pmatrix} B_{1,2} \\ D_{1,2} \end{pmatrix} \qquad (75)$$

and in the scalar SH *amplitude V*, respectively, depending on the type of interaction that is considered. In order to determine these amplitudes explicitly, we first define $P-SV$ reflectivity matrices $\mathbf{R}^-$ for the part $z > z_m$ of the medium and $\mathbf{R}^+$ for the part $z \leq z_m$ and, likewise, scalar SH reflectivities R^- and R^+ (see Fig. 3). $\mathbf{R}^-$, R^-, $\mathbf{R}^+$, R^+ are reflectivities of the type specified by Eq. (32), (40), (45) and (49), respectively. The practical computation of these quantities should be clear from the details that have been given in Section 3.

In the $P-SV$ case, the amplitude vectors $\mathbf{V}_{1,2}$ are:

$$\mathbf{S}_{1,2}^u \quad \text{for the direct wave field } (\nearrow),$$
$$\mathbf{R}^-\mathbf{R}^+\mathbf{S}_{1,2}^u \quad \text{for the first multiple of the direct wave field } (\wedge\!\!\nearrow),$$
$$\mathbf{R}^-\mathbf{R}^+\mathbf{R}^-\mathbf{R}^+\mathbf{S}_{1,2}^u \quad \text{for the second multiple } (\wedge\!\wedge\!\nearrow),$$
$$\vdots$$
$$\mathbf{R}^-\mathbf{S}_{1,2}^d \quad \text{for the reflected wave field } (\vee\!\nearrow),$$
$$\mathbf{R}^-\mathbf{R}^+\mathbf{R}^-\mathbf{S}_{1,2}^d \quad \text{for the first multiple of the reflected wave field } (\vee\!\vee\!\nearrow),$$
$$\vdots$$

The sum of all these wave fields has the amplitude vectors

$$\mathbf{V}_{1,2} = (\mathbf{I} + \mathbf{R}^-\mathbf{R}^+ + \mathbf{R}^-\mathbf{R}^+\mathbf{R}^-\mathbf{R}^+ + \ldots)(\mathbf{S}_{1,2}^u + \mathbf{R}^-\mathbf{S}_{1,2}^d)$$
$$= [\mathbf{I} - \mathbf{R}^-\mathbf{R}^+]^{-1}(\mathbf{S}_{1,2}^u + \mathbf{R}^-\mathbf{S}_{1,2}^d). \qquad (76)$$

Their components [see Eq. (75)], when inserted into Eq. (74), specify the complete upgoing $P-SV$ wave field in layer m.

The corresponding SH potential is the expression for χ^u in Eq. (74) with

$$V = (1 - R^- R^+)^{-1}(S^u + R^- S^d). \tag{77}$$

Note the structural similarity of Eqs. (76) and (77).

The *second step* in the synthesis of the wave field for $z = 0$ is to determine, from the potentials (74), the potentials ϕ^0, Ψ^0 and χ^0 in the upper half-space of the layered medium and from these the displacement components at $z = 0$. The $P - SV$ amplitude vectors in the upper half-space, $\mathbf{V}^0_{1,2}$, follow from those in layer m, $\mathbf{V}_{1,2}$ in Eq. (76), by multiplication from the left with the transmissivity matrix $\mathbf{T}^+$ of the layers between $z = z_m^+$ and $z = z_1^- = 0-$ [see Eq. (54) and Fig. 3]:

$$\mathbf{V}^0_{1,2} = \begin{pmatrix} B^0_{1,2} \\ D^0_{1,2} \end{pmatrix} = \mathbf{T}^+ \mathbf{V}_{1,2}. \tag{78}$$

Then the potentials ϕ^0 and Ψ^0 are ($z \leq 0$):

$$4\pi\rho_m\phi^0 = \int_0^\infty (\varepsilon_1 B^0_1 J_0 + \varepsilon_2 B^0_2 J_1) e^{+j\omega a_0 z} du$$

$$4\pi\rho_m\Psi^0 = \int_0^\infty \frac{1}{ju\omega}(\varepsilon_1 D^0_1 J_0 + \varepsilon_2 D^0_2 J_1) e^{+j\omega b_0 z} du. \tag{79}$$

The SH potential is, accordingly,

$$4\pi\rho_m\chi^0 = \int_0^\infty \eta\, T^+ V J_1 e^{+j\omega b_0 z} du \tag{80}$$

with V from Eq. (77), and with the scalar transmissivity T^+ defined in the same way as $\mathbf{T}^+$. The calculation of $\mathbf{T}^+$ and T^+ is performed with Eqs. (46) and (50), respectively; in these formulas the index n is replaced by m.

The displacement components follow from inserting Eqs. (79) and (80) into Eq. (6) and (6'), respectively. The results are given below for far-field and near-field terms separately. They can be written in a compact form, if the following definitions are used:

$$\mathbf{U} = \begin{pmatrix} u & b_0 \\ a_0 & -u \end{pmatrix}, \quad \mathbf{u} = \begin{pmatrix} u \\ b_0 \end{pmatrix} \tag{81}$$

$$\mathbf{J_1} = \begin{pmatrix} -J_1(u\omega r) & 0 \\ 0 & jJ_0(u\omega r) \end{pmatrix},$$

$$\mathbf{J_2} = \begin{pmatrix} J_0(u\omega r) & 0 \\ 0 & jJ_1(u\omega r) \end{pmatrix} \tag{82}$$

The vector $\mathbf{u}$ should not be confused with the displacement vector. The *far-field displacements* at the level $z = 0$ are

$$4\pi\rho_m \begin{pmatrix} u_r^{ff} \\ u_z^{ff} \end{pmatrix} = \omega \sum_{i=1}^2 \varepsilon_i \int_0^\infty \mathbf{J_i U T^+ V_i}\, du$$

$$\mathbf{V_i} = [\mathbf{I} - \mathbf{R^- R^+}]^{-1}(\mathbf{S_i^u} + \mathbf{R^- S_i^d}) \tag{83}$$

$$4\pi\rho_m u_\varphi^{ff} = -\omega\eta \int_0^\infty J_0(u\omega r) u\, T^+ V du$$

$$V = (1 - R^- R^+)^{-1}(S^u + R^- S^d). \tag{84}$$

The *near-field displacements* are:

$$4\pi\rho_m \begin{pmatrix} u_r^{nf} \\ u_\varphi^{nf} \end{pmatrix}$$
$$= \begin{pmatrix} -\varepsilon_2 \\ \eta \end{pmatrix} \int_0^\infty \frac{1}{ur} J_1(u\omega r)(\mathbf{u^T T^+ V_2} + u\, T^+ V)\, du \tag{85}$$

$$u_z^{nf} = 0.$$

The *total displacement vector* is the sum of the near-field and far-field vectors. Closer inspection shows that at the origin this vector (in Cartesian coordinates) is finite and independent of φ, as it should be.

The results (83)–(85) reflect the well-known fact that, in the far field of a point source, $P - SV$ waves are restricted to the radial and the vertical component and SH waves to the transverse component. Only in the near field do $P - SV$ waves appear also on the transverse and SH waves also on the radial component. Moreover, the two terms in Eq. (83) are easily identified as the displacements due to a vertical force ($i = 1$) and a horizontal force ($i = 2$). A purely vertical force produces no near-field displacements ($\varepsilon_2 = \eta = 0$).

The results (83–(85), supplemented by the factor $e^{j\omega t}$, are the displacements due to the harmonic single force $\mathbf{F} = (F_1, F_2, F_3) \cdot e^{j\omega t}$. As they stand, they can also be considered as the Fourier transforms of the displacements due to time-dependent force components, with $F_i = F_i(\omega)$ being the Fourier transform of the i-th component. With this in mind, one obtains *time-domain displacement seismograms* by inverse Fourier transformation of Eqs. (83)–(85).

Equations (83)–(85) represent the complete displacement field of the medium, including body and surface waves, in spite of their derivation in terms of body-wave notions such as reflection, transmission, upward and downward propagation and decomposition into multiple waves. Surface waves in the sense of normal modes are related to poles of the integrands on the positive real u-axis which follow from the *dispersion equations*:

$$\det[\mathbf{I} - \mathbf{R^- R^+}]^{-1} = 0 \quad \text{(Rayleigh waves)}$$
$$1 - R^- R^+ = 0 \quad \text{(Love waves)}. \tag{86}$$

Further theoretical discussion of these equations and how they are solved for the slowness-frequency relation of Rayleigh and Love waves can be found in Kennett (1983). Here, where the interest is concentrated on the calculation of theoretical seismograms, it is sufficient to remark that the poles of the integrands are shifted away from the real u-axis if absorption is introduced via complex wave velocities (see Section 6.2). Hence, straightforward numerical integration of Eqs. (83)–(85) poses no problem in principle and both body- and surface-wave contributions to theoretical seismograms are obtained. It is, of course, possible to calculate only body *or* surface waves by integrating only over the corresponding slownesses.

4.4 Exact results for a free surface

The displacements (83)–(85) were derived for the case that the layered medium has a homogeneous upper half-

space with non-zero velocities α_0, β_0 and density ρ_0. Realistic seismogram calculations, corresponding to a free surface $z = 0$, can probably be performed by choosing α_0 and ρ_0 approximately as the values of air, and $\beta_0 \ll \alpha_0$. It is more elegant, however, to obtain exact free-surface conditions by the limiting process $\alpha_0 \to 0$, $\beta_0 \to 0$, $\rho_0 \to 0$. The parameters α_0, β_0, ρ_0 appear in the matrix $\mathbf{U}$, in the vector $\mathbf{u}$ [see Eq. (81)] and in the transmissivities $\mathbf{T^+}$ and T^+. The transmissivities follow from Eqs. (46) and (50), respectively, with the index n replaced by the index m of the layer with the source (see Fig. 3):

$$\mathbf{T^+} = \mathbf{T_1^u G}, \qquad \mathbf{G} = \mathbf{G_1 G_2 \ldots G_{m-1}} \qquad (87)$$

$$T^+ = t_1^u G, \qquad G = G_1 G_2 \ldots G_{m-1}. \qquad (88)$$

$\mathbf{T_1^u}$ is the matrix of $P-SV$ transmission coefficients of the interface $z = z_1 = 0$ for wave incidence from below, as defined in Eq. (25), and t_1^u is the corresponding SH transmission coefficient. These coefficients follow from Table 2 by changing the half-space index 1 to 0 and the index 2 to 1. Only in $\mathbf{T_1^u}$ and t_1^u do the parameters α_0, β_0, ρ_0 appear; $\mathbf{G}$ and G are free of them.

We then introduce in the $P-SV$ case the new quantities

$$2\mathbf{H} = \mathbf{U T_1^u}, \qquad 2\mathbf{h^T} = \mathbf{u^T T_1^u},$$

and perform in them and in t_1^u the limiting process $\alpha_0 \to 0$ (hence $a_0 \to \infty$), $\beta_0 \to 0$ (hence $b_0 \to \infty$) and $\rho_0 \to 0$. At first sight this does not look trivial in the $P-SV$ case, but actually it is simple since only terms which contain the product $a_0 b_0$ have to be taken into account. We obtain:

$$\mathbf{H} = \frac{1}{(1 - 2\beta_1^2 u^2)^2 + 4\beta_1^4 u^2 a_1 b_1}$$
$$\cdot \begin{pmatrix} 2\beta_1^2 u a_1 b_1 & (1 - 2\beta_1^2 u^2) b_1 \\ (1 - 2\beta_1^2 u^2) a_1 & -2\beta_1^2 u a_1 b_1 \end{pmatrix} \qquad (89)$$

$\mathbf{h^T} = $ first row of $\mathbf{H}$

$t_1^u = 2$.

Then the following substitutions are made in Eqs. (83)–(85):

$$\mathbf{U T^+} = 2\mathbf{H G}, \qquad \mathbf{u^T T^+} = 2\mathbf{h^T G}, \qquad T^+ = 2G. \qquad (90)$$

$\mathbf{G}$ and G are defined by Eqs. (87) and (88), respectively, and calculated with the aid of Eqs. (47) and (51).

Equations (83)–(85) together with Eq. (90) are the final results for the exact free-surface response of a layered half-space to excitation by a single force.

In their essential structure our $P-SV$ results are simpler than the forms presented in Kennett [1983, Eqs. (7.36) and (7.53)]. These forms contain a slightly different transmissivity from our results and require the calculation of a third reflectivity matrix in addition to $\mathbf{R^-}$ and $\mathbf{R^+}$. The relative simplicity of the form obtained here will probably also imply some savings in computing time. We mention also that the above special treatment of the free surface $z = 0$ leads to results which appear to be identical in structure with the results of Luco and Apsel (1983), whose approach starts *directly* with the free-surface boundary conditions.

4.5 Results for a moment-tensor point source

A generalized point source is represented by the symmetric moment tensor

$$\mathbf{M} = \begin{pmatrix} M_{11} & M_{12} & M_{13} \\ M_{12} & M_{22} & M_{23} \\ M_{13} & M_{23} & M_{33} \end{pmatrix}. \qquad (91)$$

This tensor represents a superposition of three single couples without moment along the x-, y- and z-axes of the Cartesian coordinate system introduced earlier and three double couples in the xy-, xz- and yz-planes. The tensor components may be frequency dependent. The moment-tensor point source includes, as special cases, simpler point sources such as an explosion or a double couple of arbitrary orientation; it does not include single forces.

For instance, an explosion in layer m, having the reduced displacement potential $F(t)$, is represented by Eq. (91) with vanishing mixed components and

$$M_{11} = M_{22} = M_{33} = -4\pi \rho_m \alpha_m^2 \bar{F}(\omega), \qquad (92)$$

where $\bar{F}(\omega)$ is the Fourier transform of $F(t)$ (Müller, 1973). For a double couple of arbitrary orientation, specified by two orthogonal unit vectors $\mathbf{f}$ and $\mathbf{n}$ and by the moment function $M(t)$, the moment tensor components are

$$M_{ij} = -\bar{M}(\omega)(f_i n_j + f_j n_i), \qquad (93)$$

where $\bar{M}(\omega)$ is the Fourier transform of $M(t)$. The vectors $\mathbf{f}$ and $\mathbf{n}$ are nodal-plane normals and have between them a quadrant with P-wave motions *towards* the focus.

The wave field of each of the couples, combined in Eq. (91), is found by spatial differentiation of the wave fields of a single force with respect to the source coordinates. Details are omitted here; they can be found in the text books mentioned in the introduction. In this way source displacement potentials similar to Eqs. (58)–(60), representing a moment tensor in its general form (91), can be found. The subsequent treatment, leading to the displacements at the top of the layered medium, is exactly the same as in the case of the single force.

In the following we give first the results for the *far-field displacements* at $z = 0$ in a form similar to Eqs. (83) and (84):

$$2\pi \rho_m \begin{pmatrix} u_r^{ff} \\ u_z^{ff} \end{pmatrix} = \omega^2 \sum_{i=1}^{3} \kappa_i \int_0^\infty \mathbf{j_i} \, \mathbf{U T^+ V_i} \, du$$
$$\mathbf{V_i} = [\mathbf{I} - \mathbf{R^- R^+}]^{-1} (\mathbf{s_i^u} + \mathbf{R^- s_i^d}) \qquad (94)$$

$$2\pi \rho_m u_\varphi^{ff} = \omega^2 \sum_{i=1}^{2} \lambda_i \int_0^\infty j_i u \, T^+ V_i \, du$$
$$V_i = (1 - R^- R^+)^{-1} (s_i^u + R^- s_i^d). \qquad (95)$$

In these equations we have:

$$\kappa_1 = \tfrac{1}{2}(M_{11}\cos^2\varphi + M_{22}\sin^2\varphi + M_{12}\sin 2\varphi),$$
$$\kappa_2 = \tfrac{1}{2}M_{33}, \qquad \kappa_3 = M_{13}\cos\varphi + M_{23}\sin\varphi,$$
$$\lambda_1 = \tfrac{1}{2}(M_{11}-M_{22})\sin 2\varphi - M_{12}\cos 2\varphi, \qquad (96)$$
$$\lambda_2 = M_{13}\sin\varphi - M_{23}\cos\varphi$$

$$\mathbf{j_1} = \mathbf{j_2} = \mathbf{J_1},$$
$$\mathbf{j_3} = \mathbf{J_2}\ [\mathbf{J_{1,2}}\ \text{from Eq. (82)}] \qquad (97)$$
$$j_1 = J_1(u\omega r), \qquad j_2 = -J_0(u\omega r).$$

The source amplitudes are [e_α and e_β from Eq. (67)]:

$$\mathbf{s_1^u} = \begin{pmatrix} \dfrac{ju^3}{a_m}e_\alpha^{-1} \\ ju^2\,e_\beta^{-1} \end{pmatrix}, \qquad \mathbf{s_2^u} = \begin{pmatrix} ju\,a_m e_\alpha^{-1} \\ -ju^2\,e_\beta^{-1} \end{pmatrix},$$

$$\mathbf{s_3^u} = \begin{pmatrix} -u^2\,e_\alpha^{-1} \\ (2u^2-\beta_m^{-2})\dfrac{u}{2b_m}e_\beta^{-1} \end{pmatrix}$$

$$\mathbf{s_1^d} = \begin{pmatrix} \dfrac{ju^3}{a_m}e_\alpha \\ -ju^2\,e_\beta \end{pmatrix}, \qquad \mathbf{s_2^d} = \begin{pmatrix} ju\,a_m e_\alpha \\ ju^2\,e_\beta \end{pmatrix}, \qquad (98)$$

$$\mathbf{s_3^d} = \begin{pmatrix} u^2\,e_\alpha \\ (2u^2-\beta_m^{-2})\dfrac{u}{2b_m}e_\beta \end{pmatrix}$$

$$s_1^u = \frac{ju}{2\beta_m^2 b_m}e_\beta^{-1}, \qquad s_2^u = \frac{-1}{2\beta_m^2}e_\beta^{-1}$$

$$s_1^d = \frac{ju}{2\beta_m^2 b_m}e_\beta, \qquad s_2^d = \frac{1}{2\beta_m^2}e_\beta. \qquad (99)$$

The remaining quantities in Eqs. (94) and (95) are identical with those in Eqs. (83) and (84). The *near-field displacements* are:

$$2\pi\rho_m\begin{pmatrix}u_r^{nf} \\ u_\varphi^{nf}\end{pmatrix}$$
$$= \omega\int_0^\infty \left\{\begin{pmatrix}\kappa_4 \\ -\lambda_1\end{pmatrix}\frac{1}{ur}\left(J_0-\frac{2J_1}{u\omega r}\right)(\mathbf{u^T T^+ V_1}-2u\,T^+ V_1)\right.$$
$$\left.+\begin{pmatrix}-\kappa_3 \\ -\lambda_2\end{pmatrix}\frac{J_1}{ur}(\mathbf{u^T T^+ V_3}-u\,T^+ V_2)\right\}du \qquad (100)$$

$$2\pi\rho_m u_z^{nf} = j\omega\kappa_4\int_0^\infty \frac{J_1}{ur}\mathbf{v^T T^+ V_1}\,du$$

$$\kappa_4 = \tfrac{1}{2}(M_{22}-M_{11})\cos 2\varphi - M_{12}\sin 2\varphi. \qquad (101)$$

In these expressions the Bessel functions J_0 and J_1 have been written without their argument $u\omega r$, the column vector $\mathbf{v}$ has the components a_0 and $-u$, and all other quantities are the same as in Eqs. (94) and (95); the column vector $\mathbf{u}$ is defined in Eq. (81).

Exact results for a free surface follow, as in the case of a single force, by the substitutions (90) supplemented by $\mathbf{v^T T^+} = 2\mathbf{k^T G}$, where $\mathbf{k^T}$ is a row vector formed by the second row of matrix $\mathbf{H}$ in Eq. (89). Moreover, the total displacement field is regular at the origin.

5. Discussion

5.1 Partial responses

In the following discussion reference is made only to the far-field $P-SV$ displacements for a single force in the form

$$2\pi\rho_m\begin{pmatrix}u_r^{ff} \\ u_z^{ff}\end{pmatrix} = \omega\sum_{i=1}^2 \varepsilon_i\int_0^\infty \mathbf{J_i HGV_i}\,du$$
$$\mathbf{V_i} = [\mathbf{I-R^-R^+}]^{-1}(\mathbf{S_i^u + R^- S_i^d}). \qquad (102)$$

The conclusions apply, of course, also to near-field displacements, SH waves and moment-tensor sources.

Equation (102) yields, in the far-field approximation, the *complete* medium response, i.e. all possible interactions and wave types are included. Various *partial* responses are immediately evident and they may be of great practical importance. For instance, the original form of the reflectivity method is obtained by setting $\mathbf{V_i} = \mathbf{R^- S_i^d}$, i.e. by considering only downgoing waves at the source which are reflected once at the layers below, without any further reverberation between the layers above and below the source. The matrix $\mathbf{G} = \mathbf{G_1 G_2 \ldots G_{m-1}}$ with $\mathbf{G_i}$ from Eq. (47) can be calculated either exactly, in cases where multiples and conversions produced by the upgoing wave field in the layers between the source and the free surface are of interest, or with the approximation $\mathbf{G_i} = \mathbf{E_i T_{i+1}^u}$ which implies only phase shifts in the layers and transmission losses at the interfaces. Note that the reduced wave field contains the $P-P$, $SV-P$, $P-SV$ and $SV-SV$ reflections from the layers below the source which may still be more than actually desired. In this case, one introduces vanishing elements into $\mathbf{R^-}$ and possibly also into $\mathbf{T_{i+1}^u}$.

Another important partial response is obtained by choosing $\mathbf{V_i} = \mathbf{R^-}(\mathbf{R^+ S_i^u} + \mathbf{S_i^d})$. This is similar to the foregoing case but, additionally, the reflection of the source wave field at the layers above the source is included. In seismological terms this means, for instance, that besides the mantle P phase the surface reflections pP and sP at the source are also obtained. $\mathbf{R^+}$ is calculated with the aid of Eqs. (44) and (45), where n is replaced by m. Often the approximation in Eq. (44), $\mathbf{NT_{i+1}^u} = \mathbf{R_{i+1}^u} + \mathbf{T_{i+1}^d NB_i T_{i+1}^u}$ or even $\mathbf{NT_{i+1}^u} = \mathbf{R_{i+1}^u} + \mathbf{NB_i}$, is sufficient.

These brief examples of partial responses illustrate that the formalism presented here has great flexibility and that it is worthwhile to include a few such options in a computer program together with the full calculation. The flexibility of the reflectivity method is its main advantage in comparison with propagator methods which usually give the complete response of the medium. (An exception is Kind's (1985) treatment, by propagator methods, of different source and receiver structures which implies an incomplete response.)

5.2 Extended sources

Extended sources, modelled by a superposition of several point sources, will often require the use of both far- and near-field displacements. In this case it is advisable to change from cylindrical to Cartesian coordinates before the displacement fields of the individual point sources are superposed.

If the receiver distance from the source region is large compared with the source dimensions, *and if all point sources are located in the same layer m*, simple displacement formulas can be found which occasionally may be useful.

We start with the generalization of Eq. (102) and assume that the N point sources, which here are single forces, have the spectral representations $\mathbf{F}_k = (F_{1k}, F_{2k}, F_{3k})$ and act at the hypocentres (x_{sk}, y_{sk}, z_{sk}) at the times t_k (so far $t_k = 0$). Moreover, we assume the origin of the Cartesian and cylindrical coordinate systems to be directly above the source region and the receiver coordinate r to be so large that the receiver azimuth, with respect to each point source, is φ with good accuracy. Then we have from Eq. (62) $\varepsilon_{1k} = F_{3k}$ and $\varepsilon_{2k} = F_{1k} \cos \varphi + F_{2k} \sin \varphi$, and not only can the vertical displacements due to the different point sources be added, but also the horizontal radial displacements; their sum is the displacement along the azimuth direction of the receiver with good accuracy.

In the far field the Bessel functions in the matrices (82) can be replaced by the asymptotic form of the corresponding Hankel functions of the second kind, which implies that only waves propagating *away* from the source are considered. This yields:

$$\mathbf{J_{ik}} = \frac{\delta_i}{(2\pi u \omega r_k)^{1/2}} e^{-j\left(u\omega r_k - \frac{\pi}{4}\right)} \begin{pmatrix} 1 & 0 \\ 0 & -1 \end{pmatrix}, \quad (103)$$

where $\delta_1 = -j$ and $\delta_2 = 1$, and r_k is the horizontal distance from the receiver to the k-th point source; r_k in the denominator, but not in the exponential function, can be replaced by r. Finally, also the source amplitude vectors $\mathbf{S_{ik}^{u,d}}$ [see Eq. (72)] are different for different point sources: the source depth z_s in Eq. (67) has to be replaced by z_{sk}. All other quantities in Eq. (102) are independent of sources and receiver.

After some algebra, one obtains the following far-field $P - SV$ displacements for the extended source:

$$4\pi \rho_m \begin{pmatrix} u_r^{ff} \\ -u_z^{ff} \end{pmatrix} = (1-j) \left(\frac{\omega}{\pi r}\right)^{1/2} \int_0^\infty u^{1/2}\,\mathbf{HGV}\,du$$
$$\mathbf{V} = [\mathbf{I} - \mathbf{R^-R^+}]^{-1}(\mathbf{SS^u} + \mathbf{R^-SS^d}) \quad (104)$$

$$\mathbf{SS^{u,d}} = \sum_{i=1}^2 \sum_{k=1}^N \varepsilon_{ik} \mathbf{SS_{ik}^{u,d}} \quad (105)$$

$$\mathbf{SS_{1k}^{u,d}} = \frac{E}{u}\mathbf{S_{1k}^{u,d}}$$
$$\quad (106)$$

$$\mathbf{SS_{2k}^{u,d}} = j\frac{E}{u}\mathbf{S_{2k}^{u,d}}$$

$$E = \exp\{-j\omega(u r_k + t_k)\}, \quad (107)$$

$\mathbf{S_{ik}^{u,d}}$ from Eqs. (72), (66), (67) and (71) with z_s replaced by z_{sk}.

Equation (104) looks essentially like the point-source result (102) with new source amplitude vectors $\mathbf{SS^u}$ and $\mathbf{SS^d}$. These vectors are now frequency and azimuth dependent, i.e. they reflect the directivity properties of the composite source. Equation (104) is, of course, also useful for far-field calculations for only one point source $(N = 1)$.

The *SH* displacement, corresponding to the $P - SV$ displacements (104), is:

$$4\pi \rho_m u_\varphi^{ff} = -(1-j) \left(\frac{\omega}{\pi r}\right)^{1/2} \int_0^\infty u^{1/2}\,GV\,du$$
$$V = (1 - R^- R^+)^{-1}(SS^u + R^- SS^d) \quad (108)$$

$$SS^{u,d} = \sum_{k=1}^N \eta_k\,SS_k^{u,d} \quad (109)$$

$$SS_k^{u,d} = j\,ES_k^{u,d}, \quad (110)$$

E from Eq. (107), $S_k^{u,d}$ from Eq. (73), η_k from Eq. (62) for the k-th single force.

Finally, we give the far-field results for an extended source, consisting of several moment-tensor point sources. The $P - SV$ displacements are:

$$2\pi \rho_m \begin{pmatrix} u_r^{ff} \\ -u_z^{ff} \end{pmatrix} = (1-j) \frac{\omega^{3/2}}{(\pi r)^{1/2}} \int_0^\infty u^{1/2}\,\mathbf{HGV}\,du$$
$$\mathbf{V} = [\mathbf{I} - \mathbf{R^-R^+}]^{-1}(\mathbf{ss^u} + \mathbf{R^-ss^d}) \quad (111)$$

$$\mathbf{ss^{u,d}} = \sum_{i=1}^3 \sum_{k=1}^N \kappa_{ik}\,\mathbf{ss_{ik}^{u,d}} \quad (112)$$

$$\mathbf{ss_{1k}^{u,d}} = \frac{E}{u}\mathbf{s_{1k}^{u,d}}, \qquad \mathbf{ss_{2k}^{u,d}} = \frac{E}{u}\mathbf{s_{2k}^{u,d}}$$
$$\quad (113)$$

$$\mathbf{ss_{3k}^{u,d}} = j\frac{E}{u}\mathbf{s_{3k}^{u,d}},$$

$\mathbf{s_{ik}^{u,d}}$ from Eq. (98) with z_s replaced by z_{sk}.

The *SH* displacement is:

$$2\pi \rho_m u_\varphi^{ff} = -(1-j) \frac{\omega^{3/2}}{(\pi r)^{1/2}} \int_0^\infty u^{1/2}\,GV\,du$$
$$V = (1 - R^- R^+)^{-1}(s s^u + R^-\,s s^d) \quad (114)$$

$$s s^{u,d} = \sum_{i=1}^2 \sum_{k=1}^N \lambda_{ik}\,s s_{ik}^{u,d} \quad (115)$$

$$s s_{1k}^{u,d} = E s_{1k}^{u,d}, \qquad s s_{2k}^{u,d} = j\,E s_{2k}^{u,d}, \quad (116)$$

$s_{ik}^{u,d}$ from Eq. (99) with z_s replaced by z_{sk}.

The factors κ_{ik} in Eq. (112) and λ_{ik} in Eq. (115) follow from Eq. (96) for the k-th moment tensor, and E is given in Eq. (107).

The main applications of these results is in the modelling of extended earthquake sources. Such sources are represented by a sufficient number of shear dislocations or double couples with moment tensors according to Eq. (93), and these moment tensors are inserted above.

5.3 Computational aspects

Remarks on the numerical calculation of theoretical seismograms with the reflectivity method, i.e. on the calculation of integrals like Eqs. (83) and (84) or Eqs. (111) and (114), have been made by many authors (e.g. Fuchs and Müller, 1971; Kennett, 1979, 1980, 1983; Temme and Müller, 1982). So the following comments will be relatively brief.

1) The calculation of the reflectivities and transmissivities is usually the most time-consuming part in the computation, since it has to be done typically for several hundred slownesses and several ten to several hundred frequencies. The frequency-dependence is in-

troduced mainly through the phase matrices (23). The interface reflection and transmission coefficients (Tables 1 and 2) are frequency independent in the purely elastic case, but they become slightly frequency dependent if causal absorption is introduced, since then the wave velocities are frequency dependent (see Section 6.2). We found it usually sufficient to calculate these coefficients for the dominant frequency of the problem under study, such that they continue to depend only on slowness.

2) The slowness integration is performed with the trapezoidal rule and restricted to the slownesses of interest. Numerical phases with the limiting slownesses are often produced by this and they may occasionally be a serious disturbance. Their amplitudes can be reduced by application of cosine tapers at the ends of the slowness interval.

3) Fast Fourier transformation is used to go from the time domain to the frequency domain and back and the usual rules for sampling in both domains are applied. The length of the seismograms which determines the frequency interval may be very long, in particular, when the complete-response integrals are used. Then the number of frequencies may be very large. If a partial-response integral is sufficient for the problem under study, this number may be reduced.

4) In many cases it is favourable to use a reduced time scale $t - r/c - t_0$ with suitably chosen values of reduction velocity c and minimum reduced time t_0, since then the calculation starts closer to the first arrival and the seismogram length is reduced. In the frequency domain this means multiplication of the slowness integrals by the factor $e^{j\omega(r/c + t_0)}$.

5) If, in spite of these possibilities, the seismogram length has to be chosen shorter than the duration of the medium response, the resulting time-domain aliasing, i.e. appearance of late energy early in the seismogram, can be reduced or even avoided if one uses *complex* frequencies $\omega - j/\tau$ instead of ω (Bouchon, 1979). This implies, as a consequence of the damping theorem of Fourier transformation, that instead of the desired seismogram $u(t)$ the damped version $u(t)e^{-t/\tau}$ is calculated. Depending on τ, this version actually has a shorter effective length and therefore is less disturbed by time-domain aliasing. Multiplication by $e^{+t/\tau}$ gives the desired seismogram $u(t)$. τ is usually taken between 20% and 50% of the chosen seismogram length. This method often gives satisfactory results, but sometimes it does just the opposite. This happens when there would be energy in the seismogram *prior* to the time at which the computation starts; the main source of such energy are the numerical phases mentioned above. Then *blown-up* amplitudes of this energy show up late in the seismogram (after multiplication by $e^{+t/\tau}$) and they may exceed the amplitudes of the physical arrivals. Hence, the suppression of time-domain aliasing via complex frequencies cannot be performed routinely but requires special consideration in each case.

6) The reflectivity method can be programmed in such a way that efficient use can be made of modern vector computers (Sandmeier and Wenzel, 1985). According to these authors the speed of computation can be increased by a factor of 20 to 30 relative to a modern general-purpose computer; Sandmeier and Wenzel compared the CDC CYBER 205, a vector computer, and the SIEMENS 7880. Such gains in speed open up completely new possibilities in seismogram calculations for highly complicated layering and broad frequency bands.

6. Supplements

6.1 Earth-flattening transformation

Spherical earth models can be treated with the reflectivity method in the form described here after an earth-flattening transformation, i.e. the spherical earth is replaced by an equivalent or almost equivalent flat earth. Various ray and wave theoretical aspects of this transformation have been discussed by Gerver and Markushevich (1966), Biswas and Knopoff (1970), Chapman (1973) and Müller (1977a); the following is a compilation of its main features.

The depth and velocity transformation is

$$z = R \ln \frac{R}{r}, \qquad v_f(z) = \frac{R}{r} v_s(r), \tag{117}$$

where $v_s(r)$ is the P or S velocity in the spherical earth at the radial distance r from the centre, R the earth's radius, z the depth in the flat earth and $v_f(z)$ the transformed velocity. Tracing of seismic rays through both media shows that the spherical earth is mapped on a cylindrical portion of the flat earth whose radius is the epicentral distance πR of the antipode. The earth's centre is mapped on a point with infinite depth and velocities. Rays, leaving the source in both media under the same radiation angle with respect to the vertical, *always* form identical angles with the vertical at corresponding depths. They also have identical travel times with the consequence that travel-time curves, e.g. at the surface, agree. These properties characterize Eq. (117) as a high-frequency transformation.

The density transformation is not unique, but this is no serious problem since the wave amplitudes are influenced much less by the density structure than by the velocities except in the case of vertical wave propagation. In this case the wave amplitudes depend mainly on the impedance, i.e. on the velocity times density product, and therefore it is logical to make the impedances in the spherical and the flat earth identical. This yields the density transformation

$$\rho_f(z) = \frac{r}{R} \rho_s(r). \tag{118}$$

Tests show that Eq. (118) is accurate enough also for non-vertical wave propagation.

The transformations (117) and (118) are applied prior to the calculation of theoretical seismograms. This calculation is performed under the assumption that the *same* single force or moment tensor acts at the original and the transformed source, although the medium properties there are usually different. The seismograms so obtained do not yet correspond to the spherical earth. For this, they have to be multiplied, in the case of points at the surface, by the factor (see Müller, 1977a)

$$K = \left(\frac{R}{r_0}\right)^q \left(\frac{\Delta}{\sin \Delta}\right)^{1/2}, \tag{119}$$

where r_0 is the radial distance of the source from the earth's centre, Δ the epicentral distance, $q = 1$ for a single force and $q = 2$ for a moment-tensor source. The first factor in Eq. (119) serves as a correction for the differences in velocity and density at the original and the transformed source just mentioned. For deep-focus earthquakes this factor can be 1.2–1.3 and, hence, it should not be neglected in calculations of absolute amplitudes. The second factor in Eq. (119) is well-known and takes account of the different ways in which the wavefront expands in the spherical and the flat earth.

In spite of its high-frequency character, the earth-flattening transformation, Eqs. (117)–(119), has a broad range of applicability. It is useful for practically all body and surface waves travelling through the earth's mantle and also for most body waves traversing the core (e.g. Häge, 1983). Difficulties are manifest only for waves propagating very close to the earth's centre where the transformation (117) breaks down and where the velocity structure in the spherical earth, corresponding to the homogeneous-layer representation of the flat earth, oscillates strongly and hence deviates from the true structure (Müller, 1977b). In such cases, methods for synthetic seismograms, which work directly in spherical geometry, are definitely superior (e.g. Rial and Cormier, 1980).

6.2 Dissipative media

The following discussion of a way in which dissipation of wave energy can be taken into account in seismogram calculations is tailored directly to the needs of seismology. The literature on anelastic and rheological properties of earth materials is very vast. As a starting point for the interested reader, we mention only a book by Christensen (1982) on viscoelasticity in general and a review article by Minster (1980) which is geophysically oriented.

Dissipation or absorption of wave energy is often described by linear laws, i.e. it is assumed that stress and strain are linearly related as in purely elastic media. The difference to this case is that now phase shifts occur between stress and strain. This implies that the elastic moduli are no longer real, but *complex* and possibly frequency dependent. The simple one-dimensional stress-strain relation is

$$p(\omega) = M(\omega)\,\varepsilon(\omega). \tag{120}$$

If ε is a shear strain, p a shear stress, then M is identical with twice the complex rigidity μ. If ε is a volume strain or cubic dilatation, p a pressure (apart from the sign), then M is the complex bulk modulus k. As a third example, if ε is the strain along a rod or wire, p the corresponding uniaxial stress, then M is the complex Young's modulus. We will call $M(\omega)$ the *viscoelastic modulus* without specifying the mode of deformation. The general three-dimensional viscoelastic stress-strain relation of an isotropic substance is

$$p_{ij}(\omega) = [k(\omega) - \tfrac{2}{3}\mu(\omega)]\,\theta(\omega)\,\delta_{ij} + 2\mu(\omega)\,\varepsilon_{ij}(\omega), \tag{121}$$

where θ is the cubic dilatation and otherwise familiar notation has been used.

The viscoelastic modulus in Eq. (120) is separated into real and imaginary parts, $M = M_1 + jM_2$, or into magnitude and phase, $M = A e^{j\varphi}$. All these quantities in principle have to be considered as frequency dependent. The *quality factor* Q is defined by

$$Q^{-1} = M_2/M_1 = \tan \varphi. \tag{122}$$

Increasing dissipation increases the phase shift φ between stress and strain and hence decreases Q. It can be shown that, if $Q \gg 1$, Q^{-1} is proportional to the energy loss per period in a harmonic loading experiment and therefore has a simple physical meaning. Q can be measured by different techniques, including amplitude measurements of propagating waves, width measurements of spectral lines in spectra of free oscillations and, of course, phase-shift measurements between stress and strain in forced oscillations.

An important point to note is that Eq. (120), and similarly Eq. (121), can be considered as a linear filter equation. The filter, represented by the viscoelastic modulus, must be causal, i.e. the filter output $p(t)$ in the time domain must not start earlier than the filter input $\varepsilon(t)$. This requirement imposes relations between M_1 and M_2, or A and φ, which are called dispersion or Kramers–Kronig relations. Those relating magnitude A and phase φ [and hence Q, according to Eq. (122)] are the most important in the present context:

$$\ln A(\omega) = B - \frac{1}{\pi} P \int_{-\infty}^{+\infty} \frac{\varphi(\omega')}{\omega' - \omega}\,d\omega' \tag{123}$$

$$\varphi(\omega) = \frac{1}{\pi} P \int_{-\infty}^{+\infty} \frac{\ln A(\omega')}{\omega' - \omega}\,d\omega'. \tag{124}$$

Here, only Eq. (123) is needed. For simple types of frequency dependence of Q, the principal-value integral can be calculated analytically and the constant B can be determined either at high or at low frequencies. As a consequence, the viscoelastic modulus is known for all frequencies. If this procedure is followed for the rigidity $\mu(\omega)$ and the bulk modulus $k(\omega)$, and if these complex moduli are used instead of the real moduli in the solution of an *elastic* wave-propagation problem, then the frequency-domain solution of the corresponding *viscoelastic* problem is obtained. This is the *correspondence principle* of the linear theory of viscoelasticity. The time-domain solution of the viscoelastic problem follows as usual by inverse Fourier transformation.

Working with $\mu(\omega)$ and $k(\omega)$ is, however, not the procedure that is normally used. Rather, one works with wave velocities and hence replaces real velocities by *complex velocities*. For P and S waves, we have the complex velocities

$$\alpha_c(\omega) = \left[\frac{M_\alpha(\omega)}{\rho}\right]^{1/2}, \qquad \beta_c(\omega) = \left[\frac{M_\beta(\omega)}{\rho}\right]^{1/2}, \tag{125}$$

where ρ is the (real) density. The viscoelastic modulus for P waves is

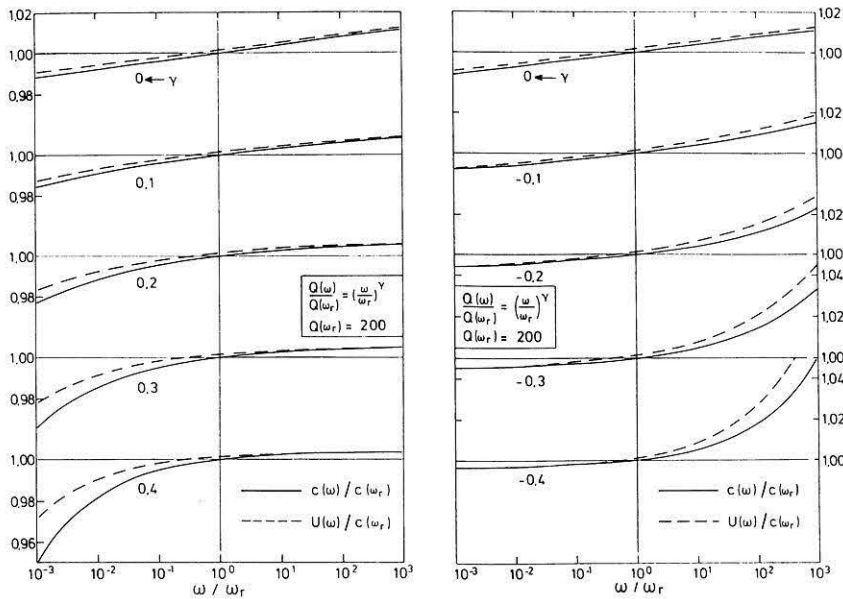$$M_\alpha(\omega) = k(\omega) + \tfrac{4}{3}\mu(\omega) \tag{126}$$

Fig. 4. Relative dispersion for phase velocity c and group velocity U of body waves, corresponding to power laws for the quality factor Q with positive and negative exponents. The case $\gamma = 0$ represents frequency-independent Q

with the quality factor Q_α following from

$$Q_\alpha^{-1} = \frac{4}{3}\frac{\beta^2}{\alpha^2} Q_\mu^{-1} + \left(1 - \frac{4}{3}\frac{\beta^2}{\alpha^2}\right) Q_k^{-1}. \tag{127}$$

For S waves we have, accordingly:

$$M_\beta(\omega) = \mu(\omega) \tag{128}$$

$$Q_\beta = Q_\mu. \tag{129}$$

Q_μ and Q_k are the quality factors of μ and k, and α and β in Eq. (127) are real wave velocities taken for a typical frequency. A familiar assumption is $Q_k \gg Q_\mu$, i.e. that there is much less dissipation in volume deformation than in shear deformation. Then Q_α depends only on Q_μ, and Q_α and Q_β have the same frequency dependence. In effect this implies a real, frequency-independent bulk modulus, at least in the seismic frequency band. An often used relation is $Q_\alpha = 2.25\, Q_\beta$, corresponding to $\alpha^2 = 3\beta^2$.

The procedure to find the complex velocities (125) is to make assumptions about Q_α and Q_β as functions of frequency, to use Eqs. (122) and (123) for the determination of M_α and M_β and then to insert these moduli into Eq. (125). In the following we will again disregard the distinction of P and S waves and work with $M(\omega)$, $Q(\omega)$ and the complex velocity

$$v_c(\omega) = \left[\frac{M(\omega)}{\rho}\right]^{1/2}. \tag{130}$$

If Q is a frequency-independent constant, or if it follows from the power law

$$Q(\omega) = Q(\omega_r)\left(\frac{\omega}{\omega_r}\right)^\gamma \tag{131}$$

with the reference frequency ω_r and an exponent γ between -1 and $+1$, the steps leading to the complex velocity (130) are rather straightforward (Müller, 1983) and will not be repeated here. These Q laws and related

absorption-band models have been investigated many times in the literature (for a review, see Minster, 1980), although often with unnecessary complications such as cut-off frequencies introduced for mathematical convenience alone. Here we give the results for the case of seismological interest, $Q \gg 1$. If Q is constant, this condition applies for all frequencies, and in the case of the power law (131) we consider only frequencies for which $Q \gg 1$. In the constant $-Q$ case one obtains the well-known result

$$v_c(\omega) = v\left(1 + \frac{1}{\pi Q}\ln\frac{\omega}{\omega_r} + \frac{j}{2Q}\right), \tag{132}$$

and in the case of the power law (131)

$$v_c(\omega) = v\left\{1 + \tfrac{1}{2}\left[\frac{1}{Q(\omega_r)} - \frac{1}{Q(\omega)}\right]\right.$$
$$\left. \cdot \cot\frac{\gamma\pi}{2} + \frac{j}{2Q(\omega)}\right\}. \tag{133}$$

In these expressions, v is a real velocity. The real part of the complex velocity,

$$c(\omega) = \mathrm{Re}\, v_c(\omega), \qquad c(\omega_r) = v, \tag{134}$$

is the phase velocity of body-wave propagation. This follows from the plane-wave expression

$$u(x,t) = \exp\left\{j\omega\left(t - \frac{x}{v_c(\omega)}\right)\right\}$$
$$\approx \exp\left\{j\omega\left(t - \frac{x}{c(\omega)\left(1 + \frac{j}{2Q}\right)}\right)\right\}$$
$$\approx \exp\left\{j\omega\left(t - \frac{x}{c(\omega)}\right)\right\}\exp\left\{-\frac{\omega x}{2c(\omega)Q}\right\}, \tag{135}$$

which represents a wave with phase velocity $c(\omega)$. The imaginary part of the complex velocity is responsible
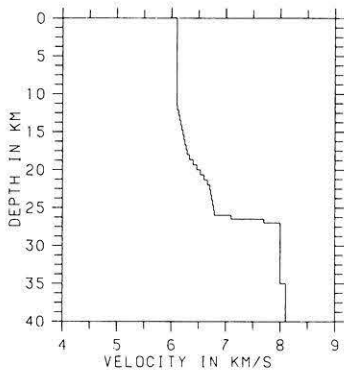
Fig. 5. P velocity-depth function of a crustal model for which theoretical seismograms are shown in Fig. 6

for absorption, since it leads to the exponential decay of the wave amplitudes in Eq. (135) with increasing propagation distance x.

The frequency dependence of $c(\omega)$ reflects the *dispersion* that is connected with absorption. Dispersion is slight, of course, and both positive and negative exponents γ lead to an increase of phase velocity with frequency (Fig. 4). Group velocity can formally be calculated from the phase velocity and has been included in Fig. 4. We have calculated synthetic seismograms for cases with relatively strong absorption and found that first-arrival times agree quite well with travel times computed from group velocity at the dominant frequency. Group velocity therefore appears to be a meaningful velocity also in the case of *weak* dispersion.

Synthetic-seismogram calculations for dissipative media with the reflectivity method require the specification of the reference frequency ω_r, the real layer velocity $c(\omega_r)$ for P and S waves, the quality factor Q or $Q(\omega_r)$ of each layer for P and S waves and the exponent

γ in the case of the power law (131). The Preliminary Reference Earth Model of Dziewonski and Anderson (1981) contains such a specification. Its reference frequency is $\omega_r = 2\pi\,\mathrm{s}^{-1}$, and Q_α and Q_β are assumed constant such that Eq. (132) applies and relates the velocities for different frequencies. O'Neill and Hill (1979) have performed seismogram calculations with the reflectivity method and Eq. (132). They compared the results with seismograms calculated for the dispersion-free, frequency-independent complex velocity

$$v_c = v\left(1 + \frac{j}{2Q}\right), \tag{136}$$

which leads to *acausal* body-wave arrivals. Therefore, this simple velocity law is not well suited for body-wave calculations, but it is often sufficient for surface waves. Incorporation of the three velocity laws (132), (133) and (136) in a computer program for theoretical seismograms offers enough possibilities for the modelling of absorption effects.

An alternative to the use of complex velocities is sometimes the use of *dissipation operators* which are convolved with seismograms, computed for purely elastic media. Dissipation operators follow from the plane-wave delta-function response of a homogeneous absorbing medium by appropriate averaging of the quality factor of an inhomogeneous medium along seismic rays. The use of such operators, normally corresponding to frequency-independent Q, is very common in conjunction with seismogram calculations by generalized or asymptotic ray theory. Operators for the power law (131) are given by Müller (1983). The use of dissipation operators, however, is restricted to body-wave investigations with little or no interference of phases propagating along different rays. Interfering body waves and surface waves usually have to be treated with the aid of complex velocities.
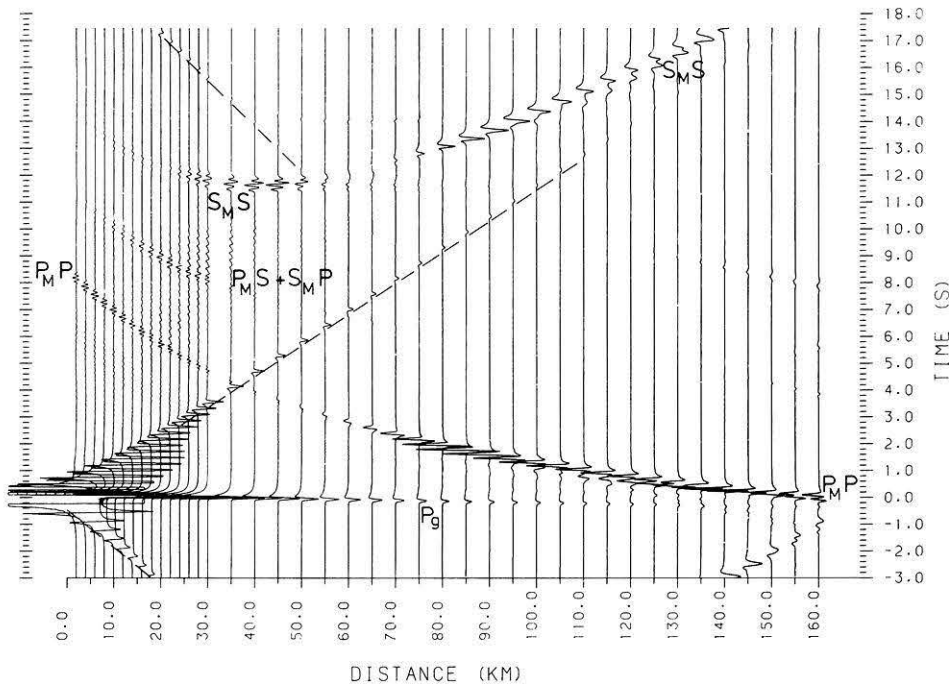

Fig. 6. Record section of vertical-component seismograms (e.g. for displacement or particle velocity), calculated for the crustal model of Fig. 5 and an explosive point source at depth 30 m. Reduction velocity is 6 km/s and true amplitudes are shown. Due to the simplicity of the crustal model, practically all seismic phases can be identified. The seismogram section also illustrates two problems that can be connected with reflectivity calculations: the appearance of numerical phases (indicated by *dashed lines*) and the occurrence of time-domain aliasing (at distances beyond 140 km)

7. Examples of theoretical seismograms

7.1 Explosion-generated body waves

The first example of theoretical seismograms consists of reflection and refraction seismological records, generated by an explosive point source in a relatively simple model of the earth's crust. The P velocities of this model are shown in Fig. 5 and the theoretical seismograms in Fig. 6. Reasonable assumptions about the S velocities and the densities were made which need not be detailed here. In the whole model, Q_α is 500 and Q_β is 250. The complex-velocity law (132) was applied, corresponding to frequency-independent Q and causal absorption. The source is at depth 30 m and radiates a far-field pulse, e.g. for displacement or particle velocity, with a dominant frequency of 5 Hz and an effective frequency band from 0 to 15 Hz; 307 frequencies were used.

The *complete* $P - SV$ response of the model was calculated with far-field expressions similar to Eqs. (104) or (111). Therefore, reflections and multiple reflections, produced by the earth's surface, are included. Due to the nature of the explosion there is no direct radiation of S waves. However, because of the proximity of the explosion to the surface, S waves are *effectively* radiated in the form of the surface reflection pS and the non-geometrical wave S^* (Hron and Mikhailenko, 1981).

The phase-velocity range in the calculation was 3.54–1,100 km/s, corresponding to the slowness window 0.0009–0.2825 s/km and including all body-wave velocities of the model; 1,300 equidistant slownesses were used. In spite of cosine tapering from 3.54 to 3.56 km/s and from 1,000 to 1,100 km/s, the amplitudes of the numerical phases, mentioned in Section 5.3, are rather strong at short distances. The Rayleigh wave tied to the surface of the model is suppressed, because its slowness falls outside the slowness window.

The theoretical seismograms in Fig. 6 show the direct wave P_g and the Moho reflections $P_M P$, $P_M S + S_M P$ and $S_M S$ as the main phases. Multiple reflections are very weak. As mentioned above, $S_M P$ and $S_M S$ actually do not leave the source as SV waves but are produced at the surface by P-to-SV conversion and S^* excitation. The amplitude behaviour of the Moho reflections is mainly determined by the reflectivities of the Moho transition. Time-domain aliasing has not been suppressed. As a consequence, $S_M S$ jumps from (correct) late arrival times to (incorrect) early arrival times at a distance of about 140 km. The reverse jump is seen in the fast numerical phase at about 20 km.

One purpose of the seismogram calculations for the crustal model of Fig. 5 and other models was to investigate quantitatively the amplitude ratio of steep-angle and wide-angle Moho reflections $P_M P$. Steep-angle reflections are strongly influenced by the special form of the velocity and density transition from the lower crust to the uppermost mantle, whereas wide-angle reflections around the critical point have more similar amplitudes. A first-order discontinuity is connected with an amplitude ratio of steep- to wide-angle reflections around 0.5. Laminated transitions, characterized by velocity and density reversals, which have been suggested several times (e.g. Fuchs, 1969; Deichmann and An-
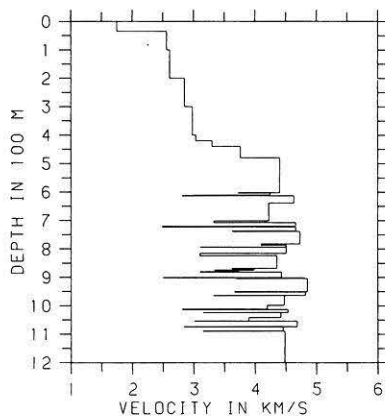

Fig. 7. P velocity-depth function of a model relevant to seismic prospecting for coal. The synthetic seismograms are shown in Fig. 8

sorge, 1983), produce even larger amplitude ratios. The observational evidence from explosion-seismological experiments is rather to the contrary, i.e. steep-angle Moho reflections appear to be considerably weaker than wide-angle reflections. This points to a Moho transition similar in character to the transition assumed in Fig. 5, with partly gradual and partly step-like velocity and density increase without pronounced lamination.

Theoretical $P - SV$ seismograms for a complicated model (Fig. 7), taken from seismic prospecting for coal, are shown in Fig. 8 as a second example. The model represents carboniferous rocks containing several groups of coal seams and overlain by a complicated overburden. The source is an explosion at depth 30 m, i.e. in the first layer. The frequency range is 0–300 Hz with a dominant frequency of 100 Hz; 307 frequencies have been used. The phase-velocity range is 1–1,100 km/s, and 1,300 slownesses are distributed over this range. Since the lowest S velocity of the model is 1.01 km/s, the seismograms include all body waves of the model, but the Rayleigh waves, connected with the waveguide formed by the first layer and represented by the low frequencies at the end of the seismograms in Fig. 8, may not be modelled completely. Q_α is 1,000 and Q_β is 500 throughout the model. Time-domain aliasing has been successfully suppressed by choosing the time τ (see Section 5.3) equal to 0.25 s; this is about 25 % of the seismogram length.

The seismograms of Fig. 8 are truly complicated records with much interference and only few phases which can be related to particular layers of the model. The band of strong amplitudes running across the record section corresponds to waves in the top layers of the overburden. The weaker energy prior to this band is due to waves that have travelled deeper through the overburden. The weak phases in the time interval 0.4–0.55 s at short distances are compressional reflections from the groups of coal seams.

7.2 Earthquake-generated surface waves

The theoretical seismograms in Fig. 9 illustrate the possibility of calculating surface waves with the reflectivity method and of obtaining absolute amplitudes, e.g.
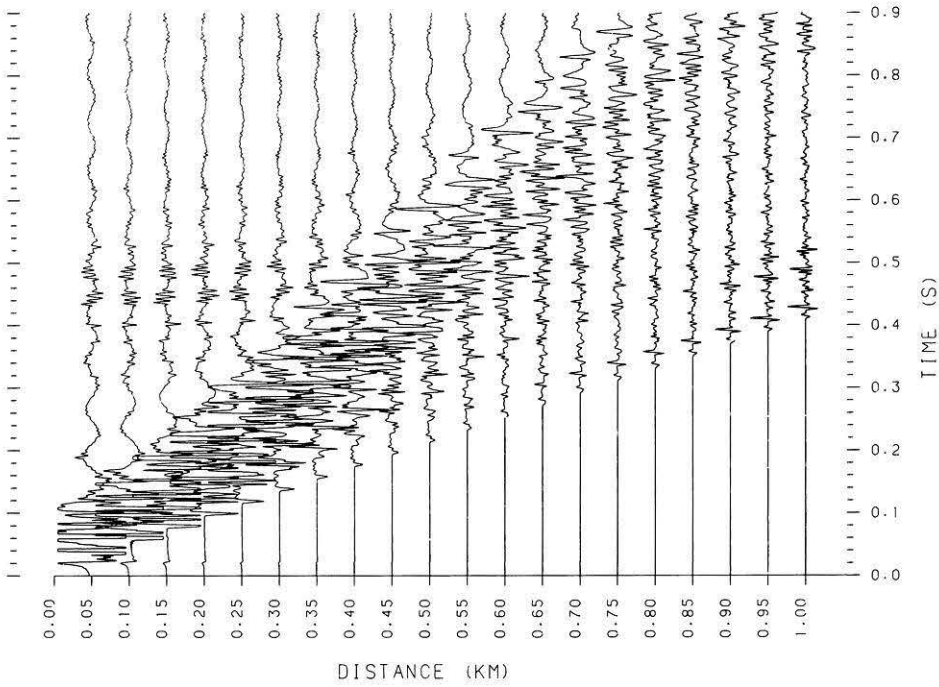
Fig. 8. Vertical-component synthetic seismograms for the model of Fig. 7. The source is an explosion at depth 30 m. True amplitudes are shown, but they are partly clipped. No travel-time reduction has been applied. A weak numerical phase with (practically) infinite phase velocity is visible at short distances
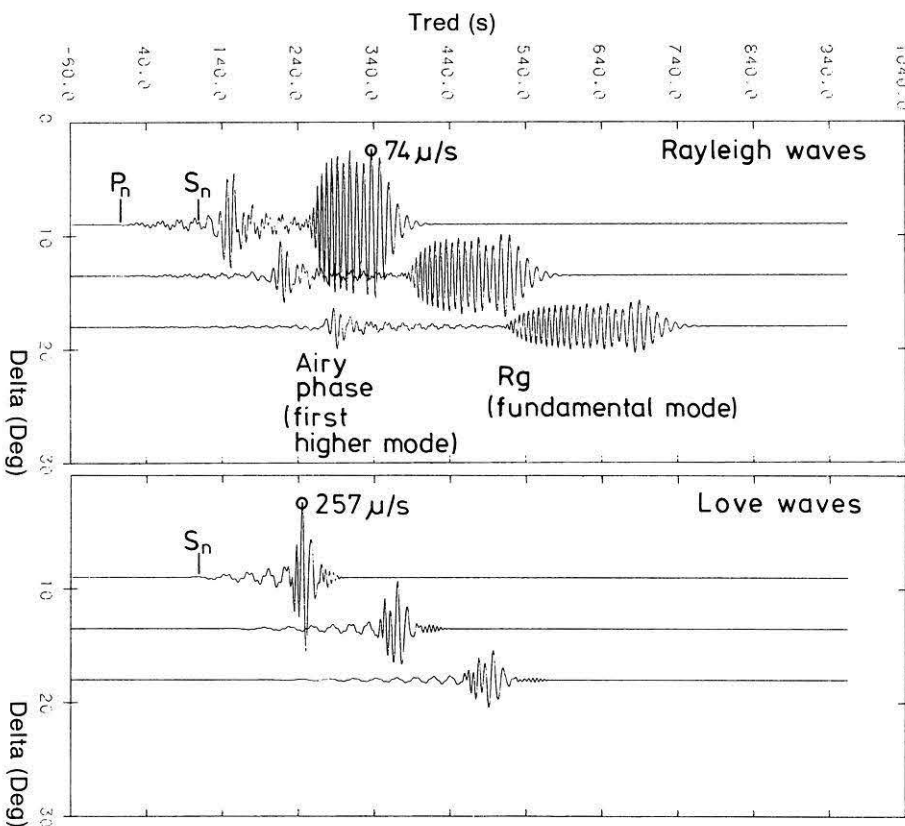

Fig. 9. Surface-wave seismograms for particle velocity; the crustal model and the source are described in the text. The Rayleigh-wave seismograms are for the vertical component, the Love-wave seismograms for the horizontal transverse component. Times are reduced with 8.1 km/s, and the theoretical P_n and S_n arrival times are indicated in the seismograms for the distance 1,000 km

for displacement or particle velocity. A simple three-layer crust-mantle model has been assumed: the layer thicknesses are $15/5/\infty$ km, the P velocities 5.0/7.2/8.1 km/s, the S velocities 2.9/4.2/4.7 km/s, the densities 2.7/3.0/3.3 g/cm³, the quality factors 700/700/225 for P waves and 300/300/100 for S waves. Thicknesses, velocities and densities were slightly modified by the earth-flattening transformation. A strike-slip

double couple is located at depth 10 km. Its moment function, whose spectrum $\bar{M}(\omega)$ enters the double-couple moment tensor (93), corresponds to the build-up of the moment 10^{25} dyne cm over a rise time of 10 s. The frequency range is 0–0.4 Hz and 400 frequencies were used. The simple complex-velocity law (136) was assumed, the phase-velocity range is 2–15 km/s and the number of slownesses 500.

The synthetic seismograms for particle velocity in Fig. 9 at epicentral distances of 1,000, 1,500 and 2,000 km were calculated with the aid of Eqs. (111) and (114), respectively. The receivers have an azimuth of 30° with respect to one of the two vertical nodal planes of the double couple. The main wave groups in Fig. 9 are surface waves, and the Love waves are much stronger than the Rayleigh waves. In both cases, the main contributions come from the fundamental and the first higher mode. The Love waves show the typical surface-wave picture, i.e. regular dispersion in the first part of the seismograms and pronounced (fundamental-mode) Airy phases. The fundamental-mode Rayleigh wave contributes the inversely dispersed R_g wave, and the first higher-mode Rayleigh wave is dominated by an Airy phase with maximum group velocity.

Seismogram calculations like those for Fig. 9 are useful, among others, for determinations of the moment and moment rise time of earthquakes from long-period seismograms. The rise time is a rough measure of the rupture duration, and an estimate of rupture length follows from it by multiplication with a reasonable value for the rupture velocity. Modelling of Love waves at distances up to 20° can be very successful, even with simple average models of the crust (Brüstle and Müller, 1983). Rayleigh waves appear to be more strongly influenced by details of the crust-mantle waveguide.

8. Conclusions

The extended form of the reflectivity method presented here will probably occupy an important place in the spectrum of synthetic-seismogram methods for vertically inhomogeneous media. The main advantage in comparison with propagator methods in their usual form (e.g. Kind, 1978; Woodhouse, 1980; Kind and Odom, 1983) is the possibility of calculating partial responses of the medium. The main advantage in comparison with wavenumber summation methods working in the time domain, e.g. the Alekseev-Mikhailenko method (Alekseev and Mikhailenko, 1980), is that absorption is easily modelled by complex wave velocities. However, the reflectivity method cannot be considered as being the optimum method in all cases. For instance, for models with *many* layers per wavelength the Alekseev-Mikhailenko method will require less computing time than the reflectivity method because the essential step, a finite-difference calculation in the depth-time domain, is independent of the model complications; whereas the corresponding step in the reflectivity method requires more computing time for more complicated models (Korn and Müller, 1983). Moreover, the Alekseev-Mikhailenko method can be formulated in the frequency domain, such that absorption is easily incorporated (Korn, 1985). Also, it remains to be seen whether the reflectivity method in the form described here requires less or more computing time than propagator methods.

References

Aki, K., Richards, P.G.: Quantitative seismology-theory and methods, vol. I and II. San Francisco: Freeman and Co. 1980

Alekseev, A.S., Mikhailenko, B.G.: The solution of dynamic problems of elastic wave propagation in inhomogeneous media by a combination of partial separation of variables and finite-difference methods. J. Geophys. **48**, 161–172, 1980

Apsel, R.J., Luco, J.E.: On the Green's functions for a layered half-space, Part II. Bull. Seismol. Soc. Am. **73**, 931–951, 1983

Ben-Menahem, A., Vered, M.: Extension and interpretation of the Cagniard-Pekeris method for dislocation sources. Bull. Seismol. Soc. Am. **63**, 1611–1636, 1973

Ben-Menahem, A., Singh, S.J.: Seismic waves and sources. New York: Springer 1981

Biswas, N.N., Knopoff, L.: Exact earth-flattening calculation for Love waves. Bull. Seismol. Soc. Am. **60**, 1123–1137, 1970

Bouchon, M.: Discrete wave number representation of elastic wave fields in three-space dimensions. J. Geophys. Res. **84**, 3609–3614, 1979

Bouchon, M.: A simple method to calculate Green's functions for elastic layered media. Bull. Seismol. Soc. Am. **71**, 959–971, 1981

Brüstle, W., Müller, G.: Moment and duration of shallow earthquakes from Love-wave modelling for regional distances. Phys. Earth Planet. Inter. **32**, 312–324, 1983

Campillo, M., Bouchon, M., Massinon, B.: Theoretical study of the excitation, spectral characteristics, and geometrical attenuation of regional seismic phases. Bull. Seismol. Soc. Am. **74**, 79–90, 1984

Chapman, C.H.: The earth. flattening transformation in body wave theory. Geophys. J.R. Astron. Soc. **35**, 55–70, 1973

Chapman, C.H.: A new method for computing synthetic seismograms. Geophys. J.R. Astron. Soc. **54**, 481–518, 1978

Christensen, R.M.: Theory of viscoelasticity – an introduction (Second ed.). New York: Academic Press 1982

Cormier, V.F.: The synthesis of complete seismograms in an earth model specified by radially inhomogeneous layers. Bull. Seismol. Soc. Am. **70**, 691–716, 1980

Cormier, V.F., Richards, P.G.: Full wave theory applied to a discontinuous velocity increase: the inner core boundary. J. Geophys. **43**, 3–31, 1977

Deichmann, N., Ansorge, J.: Evidence for lamination in the lower continental crust beneath the Black Forest (Southwestern Germany). J. Geophys. **52**, 109–118, 1983

Dziewonski, A.M., Anderson, D.L.: Preliminary reference earth model. Phys. Earth Planet. Inter. **25**, 297–356, 1981

Fuchs, K.: The reflection of spherical waves from transition zones with arbitrary depth-dependent elastic moduli and density. J. Phys. Earth **16**, Special Issue, 27–41, 1968

Fuchs, K.: On the properties of deep crustal reflectors. Z. Geophys. **35**, 133–149, 1969

Fuchs, K., Müller, G.: Computation of synthetic seismograms with the reflectivity method and comparison with observations. Geophys. J.R. Astron. Soc. **23**, 417–433, 1971

Gerver, M., Markushevich, V.: Determination of a seismic wave velocity from the travel-time curve. Geophys. J.R. Astron. Soc. **11**, 165–173, 1966

Ha, J.: Recurrence relations for computing complete P and SV seismograms. Geophys. J.R. Astron. Soc. **79**, 863–873, 1984

Häge, H.: Velocity constraints for the inner core inferred

from long-period PKP amplitudes. Phys. Earth Planet. Inter. **31**, 171–185, 1983

Harvey, D.J.: Seismogram synthesis using normal mode superposition: the locked mode approximation. Geophys. J.R. Astron. Soc. **66**, 37–69, 1981

Helmberger, D.V.: The crust-mantle transition in the Bering Sea. Bull. Seismol. Soc. Am. **58**, 179–214, 1968

Hron, F., Mikhailenko, B.G.: Numerical modeling of non-geometrical effects by the Alekseev-Mikhailenko method. Bull. Seismol. Soc. Am. **71**, 1011–1029, 1981

Ingate, S.F., Bock, G., Kind, R.: Synthesis of complete *SH* seismograms. Geophys. J.R. Astron. Soc. **75**, 261–274, 1983

Kennett, B.L.N.: Reflections, rays and reverberations. Bull. Seismol. Soc. Am. **65**, 1643–1651, 1974

Kennett, B.L.N.: Theoretical reflection seismograms for an elastic medium. Geophys. Prospecting **27**, 301–321, 1979

Kennett, B.L.N.: Seismic waves in a stratified medium II. theoretical seismograms. Geophys. J.R. Astron. Soc. **61**, 1–10, 1980

Kennett, B.L.N.: Seismic wave propagation in stratified media. Cambridge: Cambridge University Press 1983

Kennett, B.L.N., Kerry, N.J.: Seismic waves in a stratified half-space. Geophys. J.R. Astron. Soc. **57**, 557–583, 1979

Kind, R.: The reflectivity method for a buried source. J. Geophys. **44**, 603–612, 1978

Kind, R.: The reflectivity method for different source and receiver structures and comparison with GRF data. J. Geophys. **58**, 146–152, 1985

Kind, R., Odom, R.I.: Improvements to layer matrix methods. J. Geophys. **53**, 127–130, 1983

Korn, M.: Kombination von Integraltransformationen und Finiten-Differenzen-Methoden zur Berechnung der Wellenausbreitung in geschichteten Medien. Ph.D. thesis, University of Frankfurt, 1985

Korn, M., Müller, G.: Comparison of the Alekseev-Mikhailenko method and the reflectivity method. Geophys. J.R. Astron. Soc. **72**, 541–556, 1983

Luco, J.E., Apsel, R.J.: On the Green's functions for a layered half-space, Part I. Bull. Seismol. Soc. Am. **73**, 909–929, 1983

Minster, J.B.: Anelasticity and attenuation. Proceedings of Enrico Fermi International School of Physics, A. Dziewonski and E. Boschi eds.: pp. 152–212. Amsterdam: North Holland 1980

Müller, G.: Theoretical seismograms for some types of point sources in layered media. Part III: Single force and dipole sources of arbitrary orientation. Z. Geophys. **35**, 347–371, 1969

Müller, G.: Seismic moment and long-period radiation of underground nuclear explosions. Bull. Seismol. Soc. Am. **63**, 847–857, 1973

Müller, G.: Earth-flattening approximation for body waves derived from geometric ray theory-improvements, corrections and range of applicability. J. Geophys. **42**, 429–436, 1977a

Müller, G.: Correction. J. Geophys. Res. **82**, 2541–2542, 1977b

Müller, G.: Rheological properties and velocity dispersion of a medium with power-law dependence of Q on frequency. J. Geophys. **54**, 20–29, 1983

Olson, A.H., Orcutt, J.A., Frazier, G.A.: The discrete wave-number/finite element method for synthetic seismograms. Geophys. J.R. Astron. Soc. **77**, 421–460, 1984

O'Neil, M.E., Hill, D.P.: Causal absorption: its effect on synthetic seismograms computed by the reflectivity method. Bull. Seismol. Soc. Am. **69**, 17–26, 1979

Panza, G.F.: Synthetic seismograms: the Rayleigh waves modal summation. J. Geophys. **58**, 125–145, 1985

Pilant, W.L.: Elastic waves in the earth. Amsterdam: Elsevier 1979

Rial, J.A., Cormier, V.F.: Seismic waves at the epicenter's antipode. J. Geophys. Res. **85**, 2661–2668, 1980

Sandmeier, K.-J., Wenzel, F.: Synthetic seismograms for a complex crustal model. Geophys. Res. Lett. **12**, 1985 (in press)

Spudich, P., Ascher, U.: Calculation of complete theoretical seismograms in vertically varying media using collocation methods. Geophys. J.R. Astron. Soc. **75**, 101–124, 1983

Temme, P., Müller, G.: Numerical simulation of vertical seismic profiling. J. Geophys. **50**, 177–188, 1982

Wang, C.Y., Herrmann, R.B.: A numerical study of *P*-, *SV*- and *SH*-wave generation in a plane layered medium. Bull. Seismol. Soc. Am. **70**, 1015–1036, 1980

Woodhouse, J.H.: Efficient and stable methods for performing seismic calculations in stratified media. Proceedings of Enrico Fermi International School of Physics, A. Dziewonski and E. Boschi, eds.: pp. 127–151. Amsterdam: North Holland 1980